UNSTEADY MASS TRANSFER AROUND SPHEROIDAL DROPS IN POTENTIAL FLOW

LY CAM HUNG

A THESIS SUBMITTED

FOR THE DEGREE OF MASTER OF ENGINEERING

DEPARTMENT OF CHEMICAL & BIOMOLECULAR ENGINEERING

NATIONAL UNIVERSITY OF SINGAPORE

2005

Acknowledgments

As I write these acknowledgments, I sincerely want to express my deep unexpressed feelings toward the number of people to whom I am indebted.

First, I gratefully acknowledge the help of my supervisor, Dr Moshe Favelukis, who has guided me through the researching process and given me professional encouragement and advice over the years. He has also taught me how to use Mathematica, the best software I have known for solving symbolic work. And, I am incredibly grateful to his course, the subject of Fluid Mechanics & Heat Transfer, for its contributions to my work in the years that followed.

Second, I wish to thank my parents, my sister and brothers who have always provided unconditional love and support to me. Instead of pressuring me to achieve goals, Mum and Dad motivated me to extend myself by saying, "As long as you do your best, we'll be proud of you". They always encouraged me to pursue what I enjoyed, and provided me with the best of everything.

Next, I also extend my thanks to all my friends, without whose support I could never have written this thesis. I deeply appreciate their constant encouragement, emotional support, and valuable suggestions.

Finally, Special thanks to the National University of Singapore that has provided a beautiful office, computers, scholarship to support my work. Sincere thanks go to the administrators and the officers of the Department of Chemical and Biomolecular Engineering.

Table of Contents

Summary

The general solution for the problem of unsteady-state mass transfer in the continuous phase around axisymmetric drops of revolution developed by Favelukis and Mudunuri (2003) has been applied for two specific cases, prolate and oblate spheroid in potential flow, under the condition of high Peclet numbers. The problems have been solved analytically with the aid of Mathematica, which can deal with symbolic mathematics. This work has been accepted for publication by Chemical Engineering Science (Favelukis and Ly, 2005).

In order to solve the problems, the shape of the drop and the tangential velocity at the surface of the drop are required. The shape of the drop in terms of the eccentricity has been obtained by establishing the relations between the spheroidal coordinates system and the coordinates system of an axisymmetric body of revolution. And then, the Laplace's equation has been considered to find the tangential velocity at the surface of the drop expressed also in terms of eccentricity. The special well known case of spherical drop is deduced.

With an assumption of the resistance to mass transfer only in a thin concentration boundary layer in the continuous phase, the analytical solutions for the concentration profile, the molar flux, the concentration boundary layer thickness, and the time to reach steady-state have been obtained. The solution suggests that the total quantity of material transferred to or from the drop decreases with time and it was determined that when the dimensionless time is greater than 2, then steady-state is, in practice, obtained. Also, prolate drops attain steady-state conditions faster than oblate drops. Furthermore, as the eccentricity increases, the total quantity of material transferred to or from the drop decreases (for a prolate spheroid) and increases (for an oblate spheroid).

List of tables

List of Figures

Nomenclature

a	semi-axis of spheroid
A	surface area
b	semi-axis of spheroid
c	molar concentration
d	focus distance
D	diffusion coefficient
e	eccentricity
f	dimensionless function
F	focus of the ellipse
h	dimensionless shape function
i	imaginary number
k	mass transfer coefficient
m	function
N	molar flux
P_n	Legendre polynomial
Pe	Peclet number
Q_n	Legendre function of the second kind.

R	local radius
Re	Reynolds number
R_{eq}	equivalent radius
s	distance
Sh	Sherwood number
t	time
U	characteristic velocity
v	velocity
x	tangential or Cartesian coordinate
y	normal or Cartesian coordinate
z	Cartesian coordinate

Greek letters

δ	concentration boundary layer thickness
η	spheroidal coordinate
θ	spheroidal coordinate
λ	dimensionless time function
ϕ	function
Φ	velocity potential
ψ	stream function, spheroidal coordinate

Subscripts

max	maximum

0 at $y = 0$.

s at the surface of the drop

∞ far away from the drop

Superscripts

* dimensionless

Chapter 1:

Introduction

The problem of mass transfer between a gas bubble or a liquid drop in a continuous fluid phase is one of the most important aspects of chemical engineering science. The development of mathematical models for the problem of mass transfer is very useful and relevant to a variety of engineering technologies such as designing industrial equipments, biochemical engineering, biological and environmental processes, and industrial food processing.

For specific equipments such as bubble column reactors and fluid beds, the problem of mass transfer needs to be solved as a basic step for designs and operations. Bubble column reactors have used for a wide range of experimentation and industrial applications including absorption, bioreactions, and catalytic slurry reactions. In a bubble column, the gas rises through the liquid providing an effective mass transfer rate. Understanding the problem of mass transfer on the surface of the bubble will be useful for the design and scale-up of bubble reactors for industry. Also, fluid beds have been used widely in many industrial systems such as chemical industry fluid beds, food and dairy fluid beds, pharmaceutical fluid beds for drying, cooking, etc. One example is the

fluid bed dryer designed to dry products including food, chemical, mineral and polymer, in which the air is supplied to the bed through a special perforated distributor plate causing bubbles form and collapse within the fluidized bed of material. In short, a mathematical model for mass transfer around a bubble is very necessary for effectively designing and operating industrial equipments.

In biochemical engineering, there are many cases of transport phenomena related to gas-liquid, liquid-liquid mass transfer. Gas-liquid mass transfer mainly concerns with oxygen supply to cells in aerobic processes as the interfacial transport through the liquid boundary layer adjacent to the bubble or the cell. Other examples are the supply or removal of other gases, like methane supply parallel to oxygen supply for single-cell protein production, as well as methane removal out of solution in anaerobic wastewater treatment. For liquid-liquid systems, we can observe mass transfer in two or even multiphase systems such as extraction of pharmaceuticals using organic solvents.

Transport of energy and mass is a general and fundamental approach to study many biological and environmental processes. It can be found that the various application areas in biological engineering involve mass transfer. For example, in the mammalian system, we can see the liquid diffusion in tissue such as drug delivery, the diffusion of saline water from veins, and the diffusion of gastric juice in the stomach. In plant system, transportation of solute and water into roots by diffusion and convection is very important for plant growth. Furthermore, in biological processing, mass transfer occurs in fermentation as convective oxygen transfer form a bubble to a cell. In addition, it is

obvious that mass transfer has been studied in environmental processes for air pollution, surface water and ground water pollution, for example, dispersion of pollutants in air, dispersive movement of surface water pollutants, and so on.

The problem of mass transfer is very important for design and operation of industrial food processing, such as drying, extraction, distillation, and absorption. Many applications of mass transfer to food systems are involved in several physical, chemical, and biological food processes, such as salting, sugaring, oxygen absorption, deaeration, crystallization, and cleaning of process equipment. And, it is really important in food packaging and storage, where transfer of moisture, vapors or gases, and flavor components may influence food quality. An understanding of the mechanism of mass transfer will be helpful in maintaining the food quality.

Several analytical mass transfer solutions for the case of a thin concentration boundary layer thickness (high Peclet numbers) have been widely investigated under steady-state condition and then developed for unsteady-state condition. The key of the solutions for the mass transfer problem is to solve the continuity equation and the partial differential mass balance equation. As the simplicity of the solution, the majority of the theoretical models presented in the literature were developed under steady-state conditions, especially for the case of a spherical drop (Levich, 1962; Ruckenstein, 1964; Lochiel and Calderbank, 1964; Brid et al., 2002). One more example is the problem of mass transfer between a slender bubble and a viscous liquid in axisymmetric extensional flow studied by Favelukis and Semiat (1996). However, in practice, unsteady-state

condition can effect significantly on the operation, especially at the initial stages of the processes.

Since the problem of mass transfer is studied between a body and a continuous fluid phase around this body, the shape of the body plays an important role in solving the problem. The problem of spherical drop or bubble is known as the simplest and ideal case in which the problem can be considered in spherical coordinate system. However, there are many physical situations in which flow conditions can cause a drop to deform. Since mass transfer between a drop and a liquid is proportional to the surface area of the drop, drop deformation should be taken into account. And, the most general case developed by many authors is axisymmetric bodies of revolution in which the flow of fluid pass the axisymmetric body along its axis of revolution (Lochiel and Calderbank, 1964; Favelukis and Mudunuri 2003).

Bubbles and drops rising or falling in a stagnant fluid under the influence of gravity usually obtain the following main shapes: sphere, ellipsoid or spherical-cap, depending on the values of the governing dimensionless numbers. Under creeping flow conditions (zero Reynolds numbers) the drop is an exact sphere, however at high values of the Reynolds numbers, the ellipsoidal regime can be obtained. Ellipsoidal fluid particles can be approximated as oblate spheroids, however this approximation may not be fully correct as bubbles and drops in this regime often lack fore-and-aft-symmetry and may show shape oscillations (Clift et al., 1978).

The behavior of a fluid depends strongly on the Reynolds numbers (*Re*), laminar flow for low *Re* and turbulent flow for high *Re*. The fluid behavior may approach that of an ideal fluid which is incompressible and has zero viscosity. The flow of such an ideal fluid is called potential flow or irrotational flow, presenting two important characteristics: (1) zero vorticity, and (2) the velocity can be written as the gradient of a scalar potential called velocity potential. As a result, the velocity potential satisfies the Laplace's equation.

In a previous work, the steady-state mass transfer in the continuous phase around axisymmetric drops of revolution, at high Peclet numbers, has been theoretically studied for both low and high Reynolds numbers (Lochiel and Calderbank, 1964; see also Clift et al., 1978). General equations for the concentration profile and the molar flux for any type of axysimmetric drop were derived, with the only requirements being the shape of the drop and the tangential velocity at the surface of the drop. Recently, Favelukis and Mudunuri (2003) extended their work, by presenting general solutions for the unsteady-state problem.

At large Reynolds numbers and without flow separation, the velocity profile around a drop can be approximated by the potential velocity or inviscid flow (Leal, 1992). This method was applied by many researchers and also by Lochiel and Calderbank (1964) for their study on the steady-state mass transfer around prolate and oblate spheroidal drops in potential flow. Although ellipsoidal drops seldom adopt prolate spheroidal forms, for the sake of completeness both cases were reported in their report.

The purpose of this thesis is to provide theoretically two new unsteady mass transfer solutions for the cases of prolate and oblate spheroidal drops under potential flow. The main body of the thesis is divided into five chapters as the following brief description. Chapter one is an introduction of the thesis. Chapter two provides the mass transfer governing equations derived by solving the continuity equation and partial differential mass balance equation (Favelukis and Mudunuri, 2003). In the third chapter, the problem of unsteady mass transfer in the continuous phase around a prolate spheroid at high Peclet numbers is investigated with an introduction of the prolate spheroidal coordinate system. The shape and the tangential velocity at the surface of the prolate spheroid have been obtained. Once again, the problem has been considered for an oblate spheroid in chapter four, distributing an in-depth study of mass transfer in spheroidal system. Finally, the results have been discussed deeply and concluded in chapter five. All the calculations in this thesis have been done with the aid of Mathematica, one of the most powerful software for symbolic work, and given in the appendices.

Most of the work presented in this Thesis was done by me with the guidance of my supervisor: Dr Favelukis, who has developed the theory given in the chapter two. I have converted his solution, originally written in the coordinates of an axisymmetric body of revolution, into the prolate and oblate spheroidal coordinate system, and obtained the solutions presented in chapters three and four. My work has mainly contributed to the paper: Favelukis M., and Ly C.H., “Unsteady Mass Transfer Around Spheroidal Drops in Potential Flow”, *Chem. Eng. Sci.*, **60**, 7011-7021 (2005).

Chapter 2:

The mass transfer governing equations

Several analytical unsteady mass transfer solutions have been presented in the literature, for the case of a thin concentration boundary layer thickness (high Peclet numbers). In creeping flow (zero Reynolds numbers), Levich (1965), Ruckenstein (1967) and Chao (1969) obtained solutions for the problem of uniform flow around a spherical drop, while the case of a simple extensional flow was treated by Gupalo et al. (1978) for a spherical drop, and by Favelukis (1998) for a slender bubble. At the other asymptotic regime of potential flow (infinite Reynolds numbers), Ruckenstein (1967) and Chao (1969) presented solutions for uniform flow around a spherical drop.

In this chapter, the general solution for the unsteady mass transfer in the continuous phase around axisymmetric drops of revolution at high Peclet numbers (see, e.g. Favelukis and Mudunuri, 2003) is revisited.

Consider a stationary axisymmetric drop of revolution (see Figure 2.1). The coordinates x and y represent tangential and normal directions to the surface of the drop

respectively, where $x = 0$ is the forward stagnation point. The local radius $R(x)$ is defined as the distance from the axis of revolution to the surface of the drop.

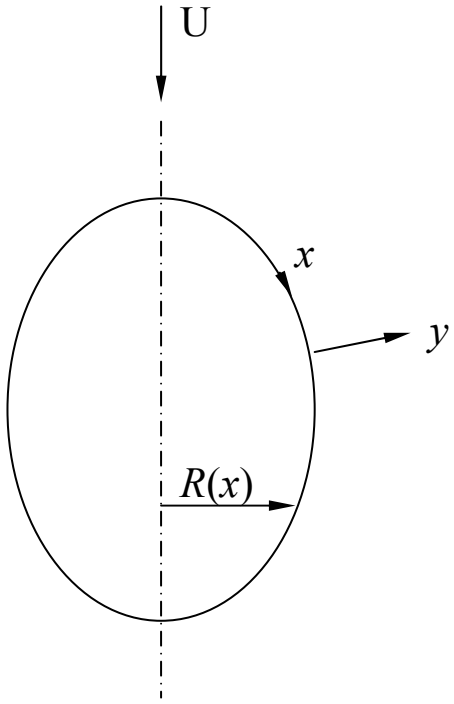

Figure 2.1: An axisymmetric drop of revolution. $R(x)$ is the local radius; x and y are the tangential and normal coordinates respectively.

The differential mass balance, in the liquid phase, for a binary axisymmetric system of constant density and diffusion coefficient (D) and assuming the thin concentration boundary layer approximation is reduced to:

$$\frac{\partial c}{\partial t} + v_x \frac{\partial c}{\partial x} + v_y \frac{\partial c}{\partial y} = D \frac{\partial^2 c}{\partial y^2} \tag{1}$$

where v_x and v_y are the disturbed velocity components, c is the molar concentration of the solute and t is the time. The above equation is solved with the following constant and uniform boundary and initial conditions:

$$c = c_s \quad \text{at} \quad y = 0 \tag{2}$$

$$c = c_\infty \quad \text{at} \quad y = \infty \tag{3}$$

$$c = c_\infty \quad \text{at} \quad x = 0 \tag{4}$$

$$c = c_\infty \quad \text{at} \quad t = 0 \tag{5}$$

The solution to the problem is obtained using the transformation $c = c(\psi, \phi)$ where $\psi = \psi(x, y)$ is the stream function and $\phi = \phi(x, t)$:

$$\frac{c - c_\infty}{c_s - c_\infty} = \operatorname{erfc}\left(\frac{\psi}{2\sqrt{\phi}}\right) \tag{6}$$

subject to the following conditions:

$$c = c_s \quad \text{at} \quad \psi = 0 \tag{7}$$

$$c = c_\infty \quad \text{at} \quad \psi = \infty \tag{8}$$

$$c = c_\infty \quad \text{at} \quad \phi = 0 \tag{9}$$

With the help of the continuity equation and the definition of the stream function, it is possible to obtain an approximate expression for the stream function, in the liquid phase, close to the surface of an axisymmetric drop of revolution:

$$\psi = v_{x0} R y \tag{10}$$

Here v_{x0} is the tangential velocity at the surface of the drop ($y = 0$) and it is a function of x only. Note that according to Eq. (10), Eqs (2) and (3) reduce to Eqs (7) and (8) respectively.

On the other hand, the function $\phi(x,t)$ can be found by the method of characteristics:

$$\phi = D \int_{m^{-1}(m-t)}^{m^{-1}(m)} v_{x0} R^2 \mathrm{d}x \tag{11}$$

where the function $m(x)$ is defined as follows:

$$m(x) = \int \frac{\mathrm{d}x}{v_{x0}} \tag{12}$$

and the notation $x = m^{-1}(m)$ is used. Note that a solution to the problem can be found only if both Eqs (4) and (5) reduce to Eq. (9) so that at $x = t = 0$, $\phi = 0$. When $t = 0$, and according to Eq. (11), this condition is always satisfied. However, this is not the case

when $x = 0$ resulting that not every physical situation can be solved by this method. Luckily, the two problems presented in this work satisfy this condition.

We define the following dimensionless parameters:

$$x^* = \frac{x}{R_{eq}} \tag{13}$$

$$y^* = \frac{y}{R_{eq}} \tag{14}$$

$$t^* = \frac{Ut}{R_{eq}} \tag{15}$$

$$v_{x0}{}^* = \frac{v_{x0}}{U} \tag{16}$$

$$R^* = \frac{R}{R_{eq}} \tag{17}$$

$$c^* = \frac{c - c_\infty}{c_s - c_\infty} \tag{18}$$

$$\psi^* = \frac{\psi}{U{R_{eq}}^2} \tag{19}$$

$$\phi^* = \frac{\phi}{DU{R_{eq}}^3} \tag{20}$$

$$A^* = \frac{A}{4\pi{R_{eq}}^2} \tag{21}$$

Here U is a characteristic velocity, R_{eq} is the equivalent radius (the radius of a sphere of an equal volume to that of the deformed drop) and A is the surface area of the drop.

The concentration profile, given by Eq. (6), can be written in a dimensionless form as:

$$c^* = \operatorname{erfc}\left(\frac{\psi^*}{2\sqrt{\phi^*}} Pe^{1/2} \right) \tag{22}$$

where Pe is the Peclet number, the ratio of convection to diffusion, defined as:

$$Pe = \frac{UR_{eq}}{D} \tag{23}$$

The instantaneous local molar flux can be written in a dimensionless form as:

$$Sh(x^*, t^*) = \frac{k(x^*, t^*)R_{eq}}{D} = \frac{1}{\sqrt{\pi}} \frac{v_{x0}{}^* R^*}{\sqrt{\phi^*}} Pe^{1/2} \tag{24}$$

here $Sh(x^*, t^*)$ is the local Sherwood number, the ratio of the total mass transfer (diffusion and convection) to the diffusional mass transfer and $k(x^*, t^*)$ is the instantaneous local mass transfer coefficient (the ratio of the instantaneous local molar flux, at the surface of the drop, to the concentration difference).

The instantaneous local concentration boundary layer thickness is given by:

$$\frac{\delta}{R} = \sqrt{\pi}\,\frac{\sqrt{\phi^*}}{v_{x0} * R^{*2}}\,\frac{1}{Pe^{1/2}} = \frac{1}{ShR^*} \tag{25}$$

where δ is the concentration boundary layer thickness (D/k). Since according to the thin concentration boundary layer approximation, the above ratio must be much smaller than 1, the following condition: $Pe^{1/2} >> 1$, must be met.

The total quantity of material transferred to or from the drop is proportional to the average flux times the surface area of the drop. In a dimensionless form, it is given by:

$$\overline{Sh}(t^*)A^* = \frac{\bar{k}(t^*)R_{\mathrm{eq}}}{D}A^* = \frac{1}{\sqrt{\pi}}\left(\int_0^{x^*_{max}} v_{x0} * R^{*2}\,\mathrm{d}x^*\right)^{1/2}\lambda(t^*)Pe^{1/2} \tag{26}$$

where $\bar{k}(t^*)$ is the instantaneous average (of position) mass transfer coefficient and the function $\lambda(t^*)$ is the ratio of the instantaneous average flux to the average flux at steady state:

$$\lambda(t^*) = \frac{\int_0^{x^*_{max}}\left(v_{x0} * R^{*2} / \sqrt{\phi^*}\right)\mathrm{d}x^*}{2\left(\int_0^{x^*_{max}} v_{x0} * R^{*2}\,\mathrm{d}x^*\right)^{1/2}} \tag{27}$$

At steady state, $\lambda(\infty) = 1$, and the final result given by Eq. (26) reduces to the useful equation derived by Lochiel and Calderbank (1964) for axisymmetric drops of revolution.

A practical estimation at short times ($t^* << 1$) that was used by many authors, can be obtained by solving Eq. (1) without the two convective terms on the left hand side:

$$\lambda(t^*) = \frac{1}{\sqrt{t^*}} \frac{\int_0^{x^*_{max}} R^* \, \mathrm{d}x^*}{2\left(\int_0^{x^*_{max}} v_{x0}^* \, R^{*2} \, \mathrm{d}x^* \right)^{1/2}} \tag{28}$$

However, we found that this estimation for short times is not correct for every physical situation and cannot be used in the present work, except for the case of a spherical drop.

Chapter 3:

Prolate spheroid

In this chapter, the problem of mass transfer will be considered in the prolate spheroidal coordinates system. As presented in the previous chapter, in order to solve the problem, the shape of the drop and the tangential velocity at the surface of the drop are required. That is the reason why the relations between the prolate spheroidal system and the coordinates of an axisymmetric body of revolution (shown in figure 2.1) should be developed. The relations between the Cartesian and the prolate spheroidal system presented by Moon and Spencer (1971) will be applied for this purpose.

3.1. Prolate spheroidal coordinates:

Figure 3.1 describes the prolate spheroidal coordinate system (η, θ, ψ) as given by Moon and Spencer (1971).

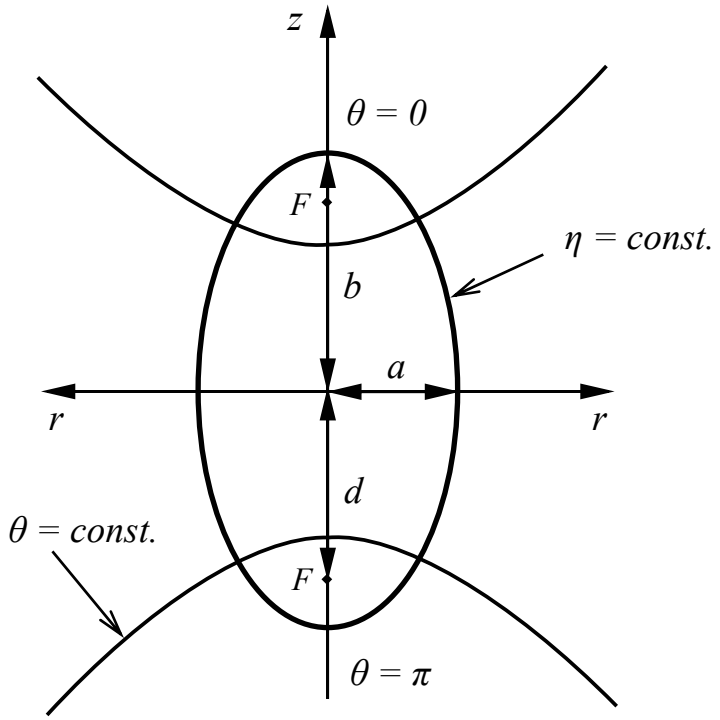

Figure 3.1: The prolate spheroidal coordinate system

The coordinate surfaces are prolate spheroids (η = constant) and hyperboloids of revolution (θ = constant). The angle ψ is not shown in the figure as it is of little interest in our axisymmetric problem. The range of the coordinates are: $0 \leq \eta < \infty$, $0 \leq \theta \leq \pi$ and $0 \leq \psi < 2\pi$. The following relations exist between the Cartesian and the prolate spheroidal system:

$$x = d\sinh\eta\sin\theta\cos\psi \tag{29}$$

$$y = d\sinh\eta\sin\theta\sin\psi \tag{30}$$

$$z = d\cosh\eta\cos\theta \tag{31}$$

where d is the distance from the origin to the focus of the ellipse (F). Note that infinity is defined in this system as $\eta = \infty$. The surface of the prolate spheroid ($\eta = \eta_0$ = constant) is described by:

$$\frac{x^2}{a^2} + \frac{y^2}{a^2} + \frac{z^2}{b^2} = 1 \tag{32}$$

Here $a = d\sinh\eta_0$ and $b = d\cosh\eta_0$ are shown in Figure 3.1 ($a \leq b$). We can define an eccentricity as follows:

$$e = \left[1 - \left(\frac{a}{b}\right)^2\right]^{1/2} \tag{33}$$

where $e = 0$ corresponds to a sphere and $e \to 1$ denotes a slender prolate spheroid. Some useful mathematical relations are: $\cosh\eta_0 = 1/e$ and $a = b(1 - e^2)^{1/2}$.

The local radius of the spheroid (see Figure 2.1) can be easily obtained from the above equations:

$$R = a\sin\theta \tag{34}$$

while the equivalent radius is defined as:

$$R_{eq} = \left(a^2 b\right)^{1/3} \tag{35}$$

Combining the last two equations we have:

$$R^* = \frac{R}{R_{eq}} = \left(1 - e^2\right)^{1/6} \sin\theta \tag{36}$$

Finally, the infinitesimal distance along the surface of the prolate spheroid is given by (Moon and Spencer, 1971):

$$\mathrm{d}s = d\left(\sinh^2\eta_0 + \sin^2\theta\right)^{1/2} \mathrm{d}\theta \tag{37}$$

In a dimensionless form and in terms of the eccentricity, we have:

$$\mathrm{d}x^* = \frac{\mathrm{d}s}{R_{eq}} = \frac{e}{\left(1 - e^2\right)^{1/3}} \left(\frac{1 - e^2}{e^2} + \sin^2\theta \right)^{1/2} \mathrm{d}\theta \tag{38}$$

3.2. Fluid mechanics:

Consider the motion of an ideal fluid with constant density and zero viscosity, a situation which can describe the flow at high Reynolds numbers. We shall review here and in section 4.2 the solution of uniform potential flow around a stationary spheroidal drop (Luiz 1967, 1969) and obtain from it the tangential surface velocity. The similar

problem of the movement of a spheroidal drop in a stagnant fluid can be found in Lamb (1945) and Batchelor (1967). Since the flow is irrotational, it follows that the velocity potential (Φ) satisfies the Laplace equation. The general solution to the Laplace equation in the prolate spheroidal coordinate system is given by (Moon and Spencer, 1971):

$$\Phi = \sum_{n=0}^{\infty}\left[A_n P_n(\cosh\eta) + B_n Q_n(\cosh\eta)\right]\left[C_n P_n(\cos\theta) + D_n Q_n(\cos\theta)\right] \tag{39}$$

where P_n are the Legendre polynomials and Q_n are the Legendre functions of second kind. Clearly that $D_n = 0$ since $Q_n(\cos\theta)$ is not defined at $\cos\theta = \pm 1$, and we may set $C_n = 1$ without loss of generality.

Consider now the problem of uniform velocity U in the $-z$ direction around a stationary prolate spheroid in potential flow. From the definition of the velocity potential in the Cartesian coordinate system, together with Eq. (31), we find that the velocity potential far away from the spheroid ($\eta \to \infty$) is:

$$\Phi = -Uz = -Ud\cosh\eta\cos\theta \tag{40}$$

From the last equation we conclude that $n = 0$ or 1, with $P_0(x) = 1$, $P_1(x) = x$, $Q_0(x) = \coth^{-1}(x)$, and $Q_1(x) = xQ_0(x) - 1$. Note that there are two definitions for $Q_0(x)$ depending on the value of x, in our case $|x| > 1$. Substituting Eq. (40) into Eq. (39) for the case where $\eta \to \infty$, results in:

$$A_1 = -Ud \tag{41}$$

From the definition of the velocity potential gradient in the prolate spheroidal coordinate system, the velocity components can be easily obtained:

$$v_\eta = \frac{1}{d\left(\sinh^2\eta + \sin^2\theta\right)^{1/2}} \frac{\partial \Phi}{\partial \eta} \tag{42}$$

$$v_\theta = \frac{1}{d\left(\sinh^2\eta + \sin^2\theta\right)^{1/2}} \frac{\partial \Phi}{\partial \theta} \tag{43}$$

At the surface of the spheroid ($\eta = \eta_0$) the normal velocity (v_η) must vanish, leading to: $B_0 = 0$. Also A_0 can be set to zero without any loss of generality resulting in:

$$B_1 = \frac{Ud\sinh^2\eta_0}{-\cosh\eta_0 + \sinh^2\eta_0 \coth^{-1}\left(\cosh\eta_0\right)} \tag{44}$$

By substituting Eqs (41) and (44) into Eqs (39) and (43), the tangential velocity at the surface of the prolate spheroid can be obtained:

$$v_{\theta 0} = \frac{U\sin\theta}{\left(\sinh^2\eta_0 + \sin^2\theta\right)^{1/2}\left[\cosh\eta_0 - \sinh^2\eta_0 \coth^{-1}\left(\cosh\eta_0\right)\right]} \tag{45}$$

Note that when we solve the problem of potential flow around a stationary object, the conditions of both zero normal and tangential velocities at the surface cannot be satisfied. Thus, the potential solution, close to the object, is not appropriate for a solid, however it is good for a drop or a bubble where a tangential surface velocity exists. Furthermore, if we solve the complete fluid mechanics problem (and not just the Laplace's equation), for the case of a spherical bubble, we find that the tangential surface velocity can be approximated by the potential solution plus a very small correction of $O(Re^{-1/2})$ (Leal, 1992). Thus, for all practical purposes we may take the potential solution for the tangential surface velocity as an excellent approximation at high Reynolds numbers. In a dimensionless form and in terms of the eccentricity, the last equation can be written as:

$$\frac{v_{\theta 0}}{U} = \frac{\sin\theta}{\left(1/e^2 - 1 + \sin^2\theta\right)^{1/2}\left[1/e - \left(1/e^2 - 1\right)\tanh^{-1}e\right]} \tag{46}$$

For a spherical drop, $e = 0$, and the well known result of $v_{\theta 0}/U = 3(\sin\theta)/2$ is obtained. On the other hand, for a slender prolate drop, $e \rightarrow 1$, and as expected, $v_{\theta 0}/U = 1$. The tangential surface velocity as a function of θ, for different values of the eccentricity e, is illustrated in Figure 3.2. The method presented here for the solution of the tangential surface velocity is different than the one presented by Lochiel and Calderbank (1964) based on the work of Zahm (1926).

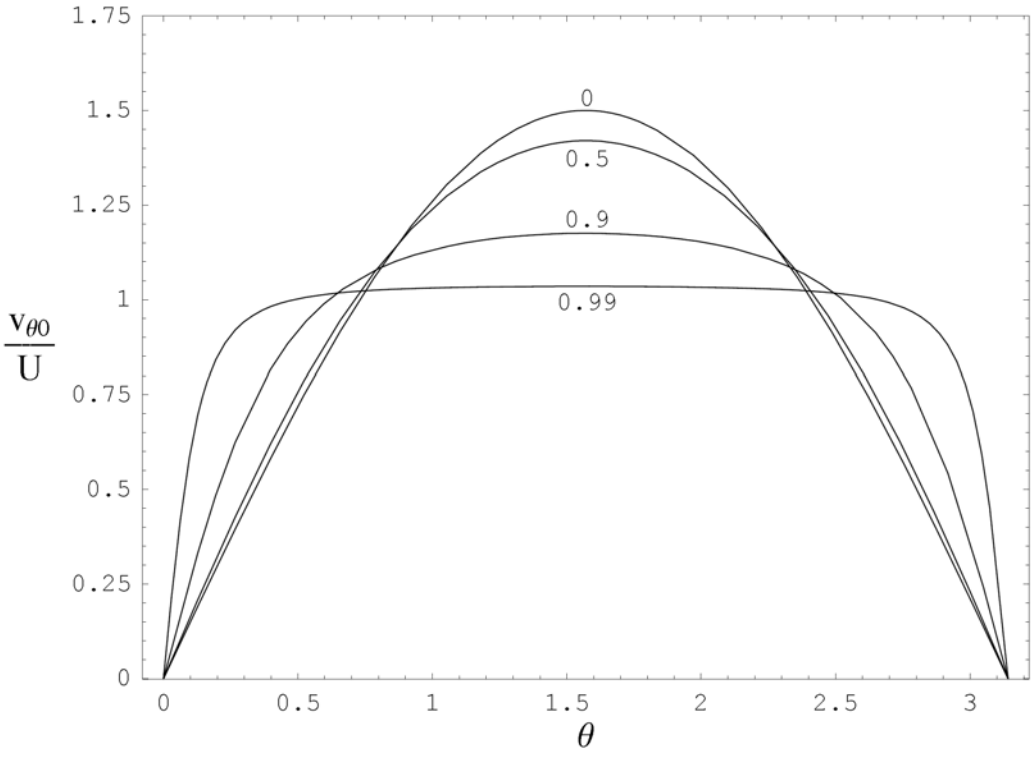

Figure 3.2: The tangential surface velocity of a prolate spheroid as a function of θ, for different values of the eccentricity e.

3.3. Mass transfer

We start this section by applying Eqs (38) and (46) in order to evaluate the functions $m(\theta)$, $m^{-1}(m)$ and $m^{-1}(m - t)$:

$$m(\theta)=\int\frac{\mathrm{d}x}{v_{x0}}=\frac{R_{eq}}{U}\frac{\left[e-\left(1-e^2\right)\tanh^{-1}e\right]}{e^3\left(1-e^2\right)^{1/3}}\left[\left(1-e^2\right)\ln\left(\tan\frac{\theta}{2}\right)-e^2\cos\theta\right] \tag{47}$$

$$\theta=m^{-1}(m)=2\tan^{-1}\left\langle\exp\left\{\frac{mU}{R_{eq}}\frac{e^3}{\left[e-\left(1-e^2\right)\tanh^{-1}e\right]\left(1-e^2\right)^{2/3}}+\frac{e^2\cos\theta}{\left(1-e^2\right)}\right\}\right\rangle \tag{48}$$

$$m^{-1}(m-t)=f(\theta,t^*)=2\tan^{-1}\left\langle \tan\frac{\theta}{2}\exp\left\{-\frac{e^3 t^*}{\left[e-\left(1-e^2\right)\tanh^{-1}e\right]\left(1-e^2\right)^{2/3}}\right\}\right\rangle \qquad (49)$$

Note that $f(0, t^*) = 0$ and $f(\theta, 0) = \theta$. The next step is applying Eqs (36), (38), (46) and (49) in order to evaluate the integral in Eq. (11). In a dimensionless form we have:

$$\phi^*(\theta,t^*)=\int_f^\theta v_{x0}^* R^{*2}\,dx^*=\frac{e^3}{12}\frac{\left[9\cos(f)-\cos(3f)-9\cos(\theta)+\cos(3\theta)\right]}{\left[e-\left(1-e^2\right)\tanh^{-1}e\right]} \qquad (50)$$

At this point one can verify that the function ϕ^* satisfies the conditions given by Eqs. (4) and (5) or (9). At steady state, $f(\theta, \infty) = 0$, the last equation reduces to:

$$\phi^*(\theta,\infty)=\frac{e^3}{12}\frac{\left[8-9\cos(\theta)+\cos(3\theta)\right]}{\left[e-\left(1-e^2\right)\tanh^{-1}e\right]} \qquad (51)$$

The local Sherwood number and the local concentration boundary layer thickness can be calculated by substituting Eqs (36), (46) and (50) into Eqs (24) and (25) to give:

$$Sh=\frac{1}{\sqrt{\pi}}\frac{\left(1-e^2\right)^{1/6}\sin^2\theta}{\left(1/e^2-1+\sin^2\theta\right)^{1/2}\left[1/e-\left(1/e^2-1\right)\tanh^{-1}e\right]}\frac{Pe^{1/2}}{\sqrt{\phi^*}} \qquad (52)$$

$$\frac{\delta}{R}=\frac{\sqrt{\pi}\left(1/e^2-1+\sin^2\theta\right)^{1/2}\left[1/e-\left(1/e^2-1\right)\tanh^{-1}e\right]}{\left(1-e^2\right)^{1/3}\sin^3\theta}\frac{\sqrt{\phi^*}}{Pe^{1/2}} \qquad (53)$$

The local Sherwood number, at different times, and for different values of the eccentricity e, is plotted in Figure 3.3

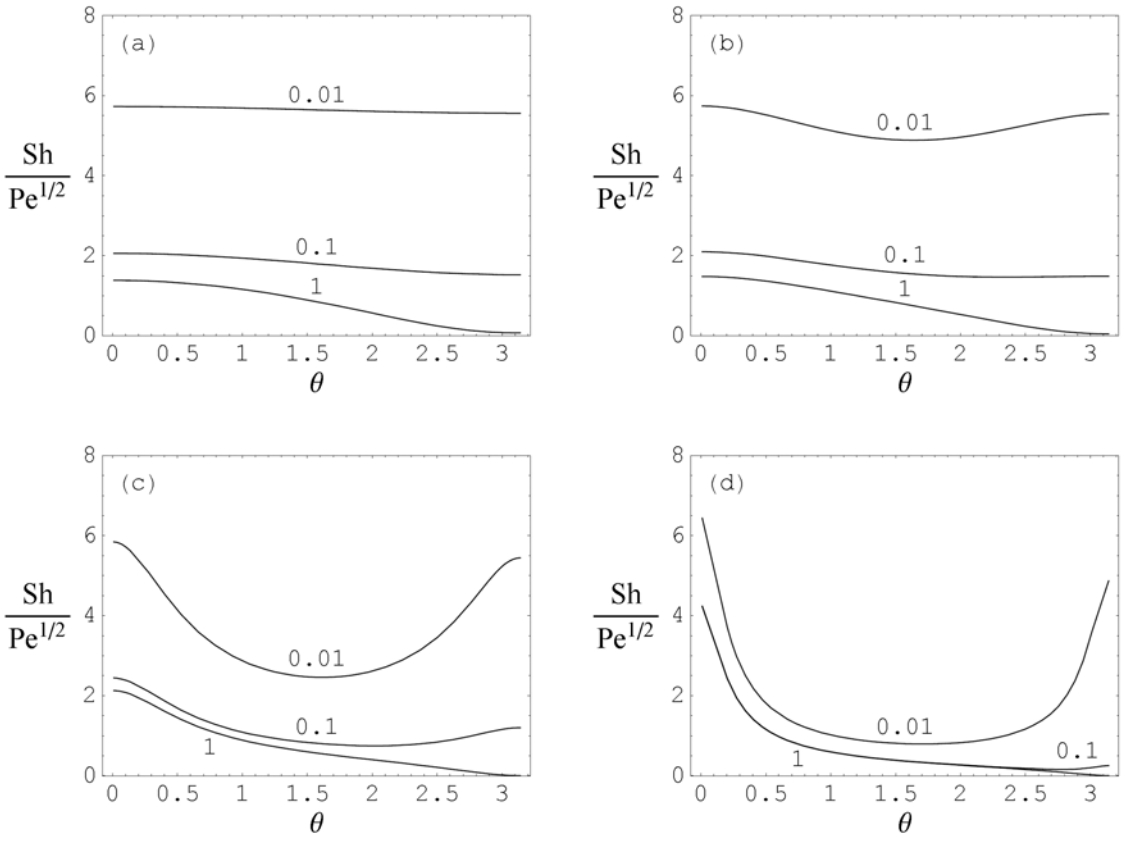

Figure 3.3: The local flux of a prolate sheroidal drop as a function of θ, at different times. (a) $e = 0$; (b) $e = 0.5$; (c) $e = 0.9$; and (d) $e = 0.99$.

At very short times, the liquid is quite clean from solute and the lines are almost symmetric around $\theta = \pi/2$. At steady-state the concentration boundary layer is cleaner from solute close to the leading edge ($\theta = 0$), and therefore there the local flux is higher, than close to the end of the drop ($\theta = \pi$) where the concentration boundary layer is contaminated with solute. It is interesting to note that, at short times, and close to the

middle of the drop ($\theta = \pi/2$), the local flux obtain a minimum. Note also that as the eccentricity increases, the local flux decreases, and it takes less time to reach steady-state conditions (see Table 3.2).

Finally, the total quantity of material transferred to or from the drop can be found from Eqs (26) and (27):

$$\overline{Sh}A^* = \sqrt{\frac{2}{\pi}}h(e)\lambda(t^*,e)Pe^{1/2} \tag{54}$$

where the dimensionless shape and time functions are given by:

$$h(e) = \sqrt{\frac{2}{3}}\left[\frac{e^3}{e-\left(1-e^2\right)\tanh^{-1}e}\right]^{1/2} \tag{55}$$

$$\lambda(t^*,e) = \frac{\sqrt{3}}{4}\left[\frac{e^3}{e-\left(1-e^2\right)\tanh^{-1}e}\right]^{1/2}\int_0^{\pi}\frac{\sin^3\theta}{\sqrt{\phi^*}}\,\mathrm{d}\theta \tag{56}$$

Some numerical values for the functions h and λ are listed in Tables 3.1 and 3.2 respectively. For a spherical drop, $e = 0$, and $h = 1$, while for a slender drop, $e \to 1$, we have $h = \sqrt{2/3}$.

e	h (prolate)	h (oblate)
0	1	1
0.2	0.9960	1.004
0.4	0.9832	1.018
0.6	0.9596	1.049
0.8	0.9186	1.128
0.99	0.8307	1.886
1	0.8165	∞

Table 3.1: Numerical values of the shape function h, according to Eqs (55) and (84).

t^*	$e = 0$	$e = 0.2$	$e = 0.4$	$e = 0.6$	$e = 0.8$	$e = 0.99$
0.001	22.36	22.15	21.46	20.08	17.32	7.295
0.01	7.072	7.004	6.786	6.351	5.477	2.319
0.1	2.250	2.229	2.162	2.027	1.761	1.019
1	1.014	1.013	1.010	1.005	1.001	1.000
2	1.000	1.000	1.000	1.000	1.000	1.000
∞	1	1	1	1	1	1

Table 3.2: Numerical values of the time function λ, according to Eq. (56) for the case of a prolate spheroid.

As expected, the total quantity of material transferred to or from the drop decreases with time, since then the boundary layer is more concentrated with solute. Furthermore, as the eccentricity increases, and the spheroid becomes more slender the value of the product $\overline{Sh}A^*$ (which is proportional to the product $h\lambda$) decreases (see Figure

3.4). Therefore, the total quantity of material transferred to or from a prolate spheroidal drop at any time is always smaller than that of a spherical drop.

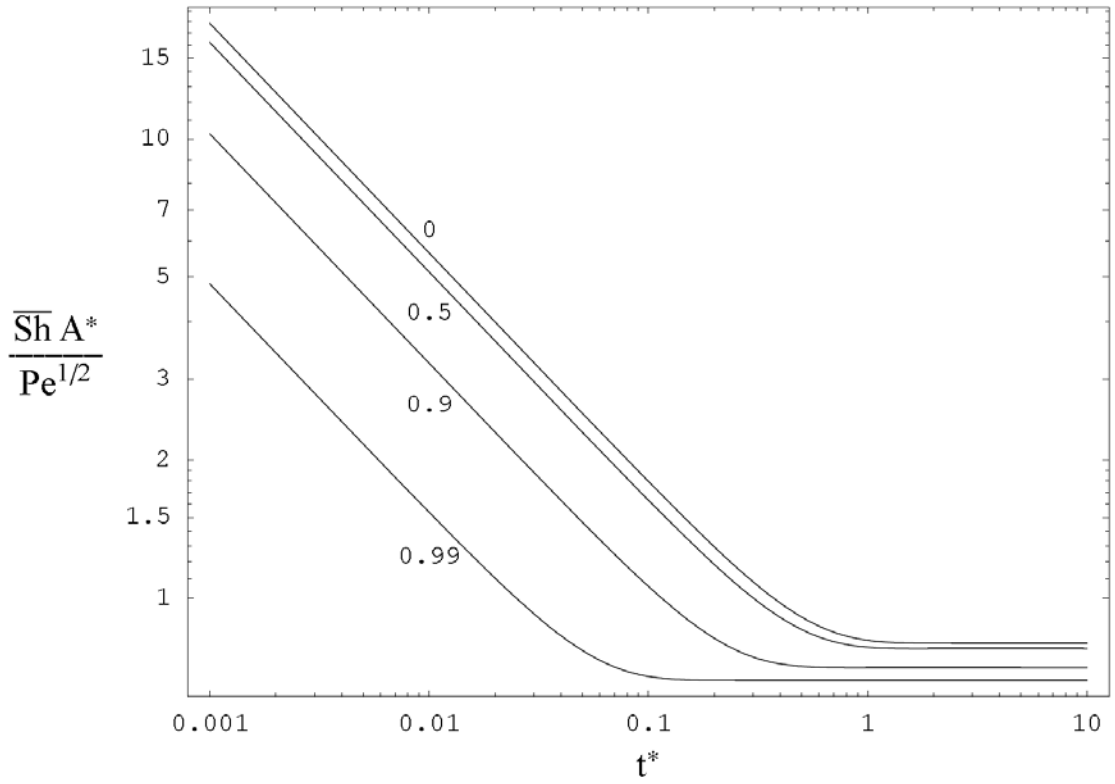

Figure 3.4: The total quantity of material transferred to or from a prolate spheroidal drop as a function of time, for different values of the eccentricity *e*.

As explained before, Eq. (28) cannot be used in the present case. However, a practical estimation at short times can be obtained by expanding Eq. (50) as a power series in time, around $t^* = 0$, and considering the first term only. After some algebraic manipulation, Eq. (56) reduces to:

$$\lambda(t^*, e) = \frac{\sqrt{3}}{2\sqrt{t^*}} \frac{\left(1-e^2\right)^{1/3}\left[e-\left(1-e^2\right)\tanh^{-1}e\right]^{1/2}}{e^{3/2}} \tag{57}$$

For the case of a sphere ($e = 0$), the last equation reduces to: $\lambda = 1/\sqrt{2t^*}$.

Chapter 4

Oblate spheroid

This chapter deals with the problem of mass transfer solved in the oblate spheroidal coordinates system. The relations between the oblate spheroidal system and the coordinates of an axisymmetric body of revolution shown in figure 2.1 will also be derived for defining the shape of an axisymmetric drop of revolution. Then, the Laplace's equation will be solved again to determine the tangential velocity at the surface of the drop, completing the requirements for solving the problem.

4.1. Oblate spheroidal coordinates

The oblate spheroidal coordinate system, (η, θ, ψ) as given by Moon and Spencer (1971), is depicted in Figure 4.1.

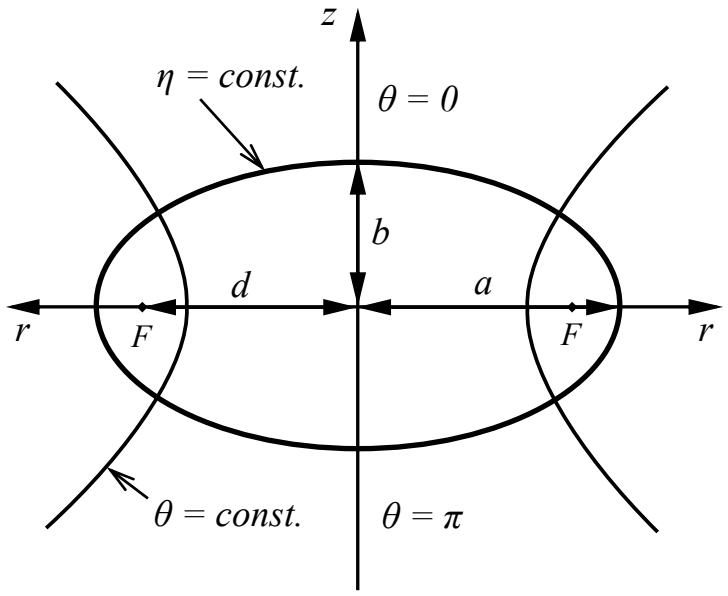

Figure 4.1: The oblate spheroidal coordinate system

Here the coordinate surfaces are oblate spheroids (η = constant) and hyperboloids of revolution (θ = constant). The ranges of the coordinates are the same as before: $0 \leq \eta < \infty$, $0 \leq \theta \leq \pi$ and $0 \leq \psi < 2\pi$. The following relations exist between the Cartesian and the oblate spheroidal coordinate system:

$$x = d\cosh\eta\sin\theta\cos\psi \tag{58}$$

$$y = d\cosh\eta\sin\theta\sin\psi \tag{59}$$

$$z = d\sinh\eta\cos\theta \tag{60}$$

As before d is the distance from the origin to the focus of the ellipse (F). Also infinity is defined as before ($\eta = \infty$). The surface of the oblate spheroid ($\eta = \eta_0$ = constant) is given by:

$$\frac{x^2}{a^2}+\frac{y^2}{a^2}+\frac{z^2}{b^2}=1 \tag{61}$$

where $a = d\cosh\eta_0$ and $b = d\sinh\eta_0$ are shown in Figure 4.1 ($a \geq b$). The eccentricity is defined somehow different this time:

$$e=\left[1-\left(\frac{b}{a}\right)^2\right]^{1/2} \tag{62}$$

Here $e = 0$ corresponds to a sphere and $e \to 1$ describes a disk. Some useful mathematical relations are: $\cosh\eta_0 = 1/e$, $a = b/(1 - e^2)^{1/2}$. Other geometrical parameters required to solve the problem are: the local and equivalent radii and the infinitesimal distance along the surface of the oblate spheroid:

$$R = a\sin\theta \tag{63}$$

$$R_{eq} = \left(a^2 b\right)^{1/3} \tag{64}$$

$$\mathrm{d}s = d\left(\cosh^2\eta_0 - \sin^2\theta\right)^{1/2}\mathrm{d}\theta \tag{65}$$

In a dimensionless form and in terms of the eccentricity, we have:

$$R^* = \frac{R}{R_{eq}} = \frac{\sin\theta}{\left(1-e^2\right)^{1/6}} \tag{66}$$

$$\mathrm{d}x^* = \frac{\mathrm{d}s}{R_{eq}} = \frac{e}{\left(1-e^2\right)^{1/6}}\left(\frac{1}{e^2}-\sin^2\theta\right)^{1/2}\mathrm{d}\theta \tag{67}$$

4.2. Fluid mechanics

The solution to the Laplace's equation in the oblate spheroidal coordinate system can be represented as (Moon and Spencer, 1971):

$$\Phi = \sum_{n=0}^{\infty}\left[A_n P_n\left(\mathrm{i}\sinh\eta\right) + B_n Q_n\left(\mathrm{i}\sinh\eta\right)\right]\left[C_n P_n\left(\cos\theta\right) + D_n Q_n\left(\cos\theta\right)\right] \tag{68}$$

where $D_n = 0$ since $Q_n(\cos\theta)$ is not defined at $\cos\theta = \pm 1$, and we may set $C_n = 1$ without loss of generality.

Consider the problem of uniform velocity U in the $-z$ direction around a stationary oblate spheroid in potential flow. Combining the definition of the velocity potential in the Cartesian coordinate system and Eq. (60) we obtain that far away from the spheroid ($\eta \to \infty$), the velocity potential reduces to:

$$\Phi = -Uz = -Ud\sinh\eta\cos\theta \tag{69}$$

The last equation suggests that $n = 0$ or 1, with $Q_0(x) = \coth^{-1}(x)$ as defined for the ordinary Legendre functions of the second kind for imaginary arguments (Abramowitz and Stegun, 1965). Combining the last two equations for the case where $\eta \to \infty$, results in:

$$A_1 = Ud\,\mathrm{i} \tag{70}$$

The velocity components, in the oblate spheroidal coordinate system, can be easily obtained from the definition of the velocity potential gradient:

$$v_\eta = \frac{1}{d\left(\cosh^2\eta - \sin^2\theta\right)^{1/2}} \frac{\partial \Phi}{\partial \eta} \tag{71}$$

$$v_\theta = \frac{1}{d\left(\cosh^2\eta - \sin^2\theta\right)^{1/2}} \frac{\partial \Phi}{\partial \theta} \tag{72}$$

At the surface of the spheroid ($\eta = \eta_0$) the normal velocity (v_η) must vanish, leading to: $B_0 = 0$. Also, A_0 can be set to zero without any loss of generality to give:

$$B_1 = \frac{Ud\cosh^2\eta_0}{-\sinh\eta_0 + \cosh^2\eta_0 \coth^{-1}\left(\sinh\eta_0\right)} \tag{73}$$

Substituting Eqs (70) and (73) into Eqs (68) and (72), the tangential velocity at the surface of the oblate spheroid can be found:

$$v_{\theta 0} = \frac{U \sin\theta}{\left(\cosh^2\eta_0 - \sin^2\theta\right)^{1/2}\left[-\sinh\eta_0 + \cosh^2\eta_0 \cot^{-1}\left(\sinh\eta_0\right)\right]} \tag{74}$$

In a dimensionless form and in terms of the eccentricity, we have:

$$\frac{v_{\theta 0}}{U} = \frac{\sin\theta}{\left(1/e^2 - \sin^2\theta\right)^{1/2}\left[-\left(1/e^2 - 1\right)^{1/2} + \left(1/e^2\right)\cot^{-1}\left(1/e^2 - 1\right)^{1/2}\right]} \tag{75}$$

For a spherical drop, $e = 0$, and the well known result of $v_{\theta 0}/U = 3(\sin\theta)/2$ is recovered. On the other hand, for a disk, $e \rightarrow 1$, no simple expression for the velocity profile can be given as it must be described by a series with many terms. The tangential surface velocity as a function of θ, for different values of the eccentricity e, is plotted in Figure 4.2.

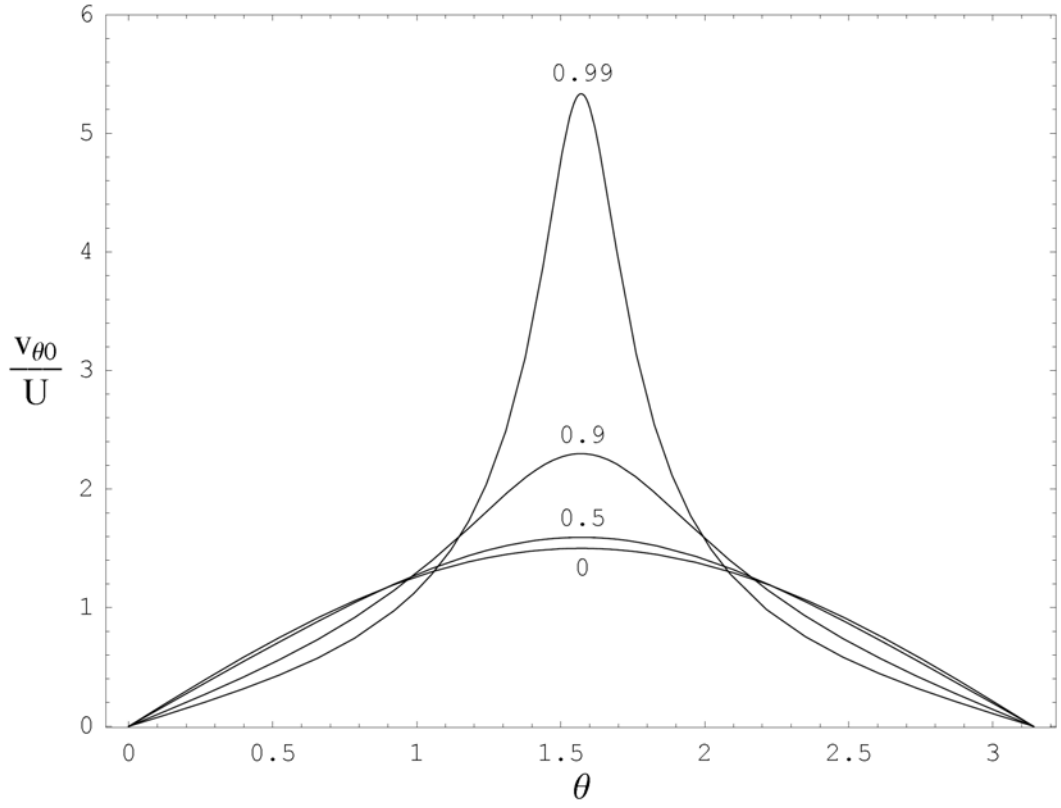

Figure 4.2: The tangential surface velocity of an oblate spheroid as a function of θ, for different values of the eccentricity e.

4.3. Mass transfer

The first step in the solution of the mass transfer problem is to obtain the functions $m(\theta)$, $m^{-1}(m)$ and $m^{-1}(m - t)$ from Eqs (67) and (75):

$$m(\theta) = \int \frac{\mathrm{d}x}{v_{x0}} = \frac{R_{eq}}{U} \frac{\left[-e\left(1-e^2\right)^{1/2} + \cot^{-1}\left(1/e^2 - 1\right)^{1/2} \right]}{e^3\left(1-e^2\right)^{1/6}} \left[\ln\left(\tan\frac{\theta}{2} \right) + e^2 \cos\theta \right] \qquad (76)$$

$$\theta = m^{-1}(m) = 2\tan^{-1}\left\langle \exp\left\{ \frac{mU}{R_{eq}} \frac{e^3\left(1-e^2\right)^{1/6}}{\left[-e\left(1-e^2\right)^{1/2} + \cot^{-1}\left(1/e^2-1\right)^{1/2}\right]} - e^2\cos\theta \right\} \right\rangle \tag{77}$$

$$m^{-1}(m-t) = f(\theta, t^*) = 2\tan^{-1}\left\langle \tan\frac{\theta}{2}\exp\left\{ -\frac{e^3\left(1-e^2\right)^{1/6} t^*}{\left[-e\left(1-e^2\right)^{1/2} + \cot^{-1}\left(1/e^2-1\right)^{1/2}\right]} \right\} \right\rangle \tag{78}$$

where $f(0, t^*) = 0$ and $f(\theta, 0) = \theta$. From Eqs (66), (67), (75) and (78), the dimensionless form of Eq. (11) can be evaluated:

$$\phi^*(\theta, t^*) = \int_f^\theta v_{x0}^* R^{*2}\, dx^* = \frac{e^3}{12} \frac{\left[9\cos(f) - \cos(3f) - 9\cos(\theta) + \cos(3\theta)\right]}{\left[-e + e^3 + \left(1-e^2\right)^{1/2}\cot^{-1}\left(1/e^2-1\right)^{1/2}\right]} \tag{79}$$

where the function ϕ^* satisfies the conditions given by Eqs. (4), (5) or (9). Under steady state conditions, $f(\theta, \infty) = 0$, and the last equation can be simplified to:

$$\phi^*(\theta, \infty) = \frac{e^3}{12} \frac{\left[8 - 9\cos(\theta) + \cos(3\theta)\right]}{\left[-e + e^3 + \left(1-e^2\right)^{1/2}\cot^{-1}\left(1/e^2-1\right)^{1/2}\right]} \tag{80}$$

The local Sherwood number and the local concentration boundary layer thickness can be calculated by substituting Eqs (66), (75) and (79) into Eqs (24) and (25) to give:

$$Sh = \frac{1}{\sqrt{\pi}} \frac{\left(1-e^2\right)^{-1/6} \sin^2\theta}{\left(1/e^2 - \sin^2\theta\right)^{1/2}\left[-\left(1/e^2-1\right)^{1/2} + \left(1/e^2\right)\cot^{-1}\left(1/e^2-1\right)^{1/2}\right]} \frac{Pe^{1/2}}{\sqrt{\phi^*}} \tag{81}$$

$$\frac{\delta}{R} = \sqrt{\pi} \frac{\left(1/e^2 - \sin^2\theta\right)^{1/2}\left[-\left(1/e^2-1\right)^{1/2} + \left(1/e^2\right)\cot^{-1}\left(1/e^2-1\right)^{1/2}\right]}{\left(1-e^2\right)^{-1/3} \sin^3\theta} \frac{\sqrt{\phi^*}}{Pe^{1/2}} \tag{82}$$

Figure 4.3 shows the local Sherwood number, at different times, for different values of the eccentricity.

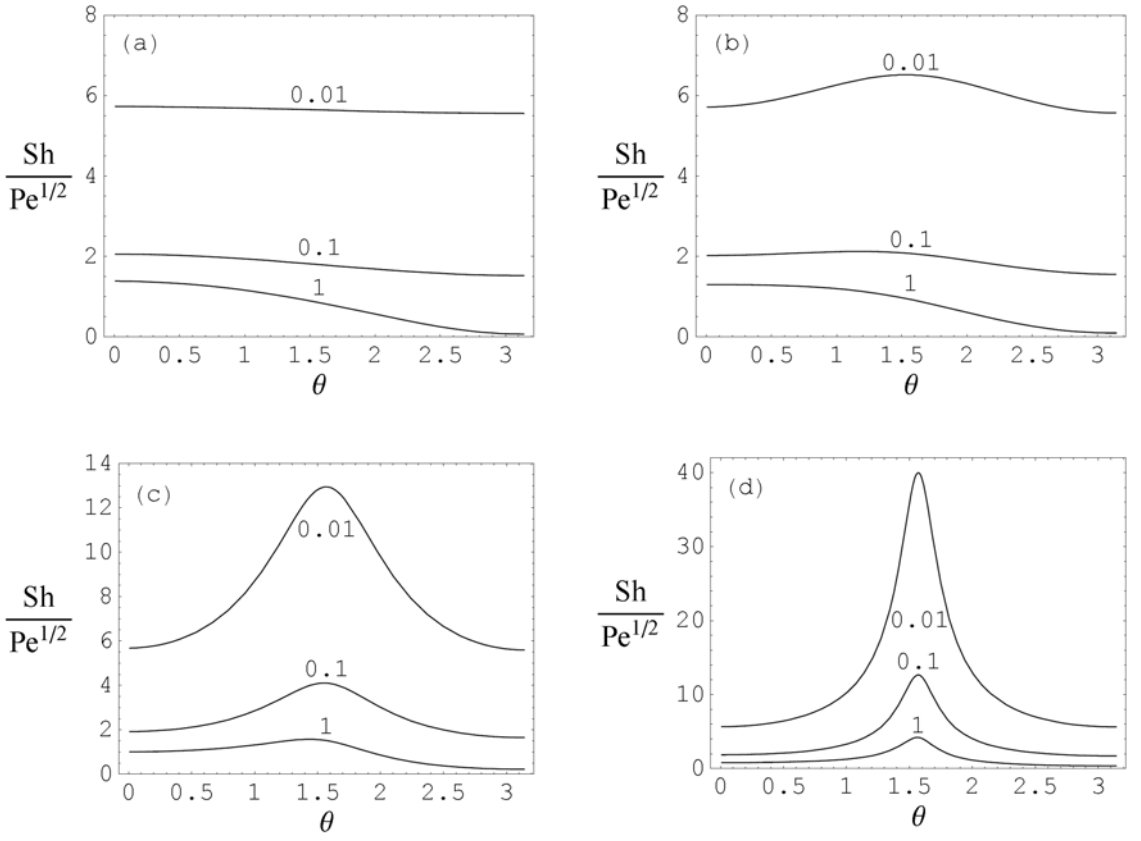

Figure 4.3: The local flux of an oblate sheroidal drop as a function of θ, at different times. (a) $e = 0$; (b) $e = 0.5$; (c) $e = 0.9$; and (d) $e = 0.99$.

Finally, we can represent the total quantity of material transferred to or from the drop, given by Eqs (26) and (27), in a similar form like the previous problem:

$$\overline{Sh}A^* = \sqrt{\frac{2}{\pi}}h(e)\lambda(t^*,e)Pe^{1/2} \tag{83}$$

where this time the shape and time functions are defined as follows:

$$h(e) = \sqrt{\frac{2}{3}}\left\{\frac{e^3}{\left[-e+e^3+\left(1-e^2\right)^{1/2}\cot^{-1}\left(1/e^2-1\right)^{1/2}\right]}\right\}^{1/2} \tag{84}$$

$$\lambda(t^*,e) = \frac{\sqrt{3}}{4}\left[\frac{e^3}{-e+e^3+\left(1-e^2\right)^{1/2}\cot^{-1}\left(1/e^2-1\right)^{1/2}}\right]^{1/2}\int_0^{\pi}\frac{\sin^3\theta}{\sqrt{\phi^*}}\,\mathrm{d}\theta \tag{85}$$

Some numerical values for the functions h and λ are listed in Tables 3.1 and 4.1 respectively. For a spherical drop, $e = 0$, and $h = 1$, while for a disk, $e \to 1$, we have $h \to \infty$. We found that the total quantity of material transferred to or from the drop decreases with time, but increases with an increase in the eccentricity, see Figure 4.4. We conclude that, the total quantity of material transferred to or from an oblate spheroidal drop at any time is always greater than that of a spherical drop.

t^*	$e = 0$	$e = 0.2$	$e = 0.4$	$e = 0.6$	$e = 0.8$	$e = 0.99$
0.001	22.36	22.57	23.28	24.73	27.87	43.76
0.01	7.072	7.139	7.361	7.820	8.814	13.84
0.1	2.250	2.271	2.340	2.483	2.794	4.378
1	1.014	1.016	1.021	1.033	1.073	1.441
2	1.000	1.000	1.000	1.001	1.004	1.127
∞	1	1	1	1	1	1

Table 4.1: Numerical values of the time function λ, according to Eq. (85) for the case of an oblate spheroid.

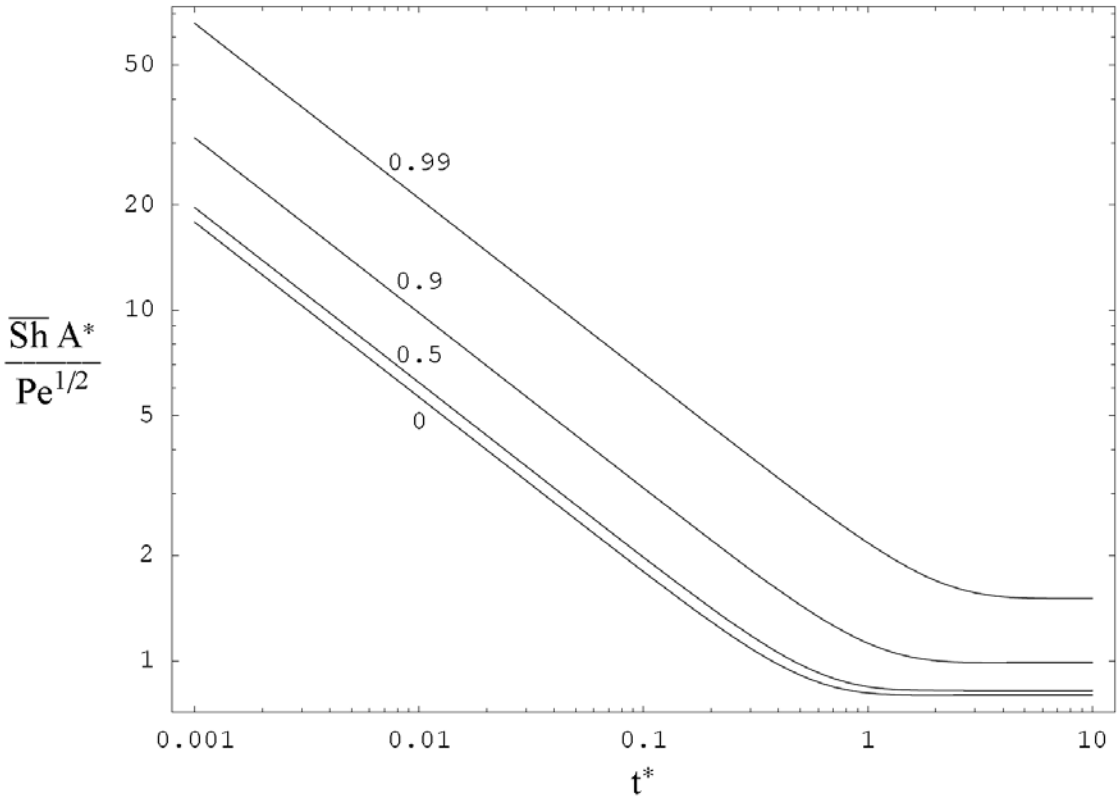

Figure 4.4: The total quantity of material transferred to or from an oblate spheroidal drop as a function of time, for different values of the eccentricity e.

Finally a practical estimation at short times can be obtained by applying the same procedure as in the previous problem:

$$\lambda(t^*, e) = \frac{\sqrt{3}}{2\sqrt{t^*}} \frac{\left[-e\left(1-e^2\right)^{1/2} + \cot^{-1}\left(1/e^2 - 1\right)^{1/2} \right]^{1/2}}{e^{3/2}\left(1-e^2\right)^{1/12}} \tag{86}$$

For the case of a sphere ($e = 0$), the last equation simplifies again to: $\lambda = 1/\sqrt{2t^*}$.

Chapter 5:

Conclusions and recommendations

The problem of unsteady mass transfer around prolate and oblate spheroidal drops in potential flow has been theoretically studied. Assuming that the resistance to mass transfer is only in a thin concentration boundary layer in the continuous phase, analytical solutions for the concentration profile, the molar flux, the concentration boundary layer thickness, and the time to reach steady-state have been obtained.

The solution method applied was derived by Favelukis and Mudunuri (2003) for axisymmetric drops of revolution, with the only requirements being the shape of the drop and the tangential velocity at the surface of the drop as shown in chapter 2. The shape of the drop can be obtained easily from the relationships between the spheroidal system and the coordinates of an axisymmetric body of revolution, and expressed in dimensionless form and in terms of eccentricity (e). In addition, the tangential velocity at the surface of the drop has been derived by solving Laplace's equation, and expressed in terms of eccentricity (e). As expected, the well known result of $v_{\theta 0}/U = 3(\sin\theta)/2$ is recovered for a spherical drop, $e = 0$. For both cases of prolate and oblate spheroid, the tangential

velocities at the surface of the drop increase with θ from 0 to $\pi/2$, being maximum at $\theta = \pi/2$, and then decreasing from $\pi/2$ to π. And when the eccentricity (e) increases in prolate spheroid or decreases in oblate spheroid, the lower of the maximum tangential velocity at $\theta = \pi/2$ has been obtained.

The local Sherwood number and the local concentration boundary layer thickness have been calculated. At short time, and close to the middle of the drop ($\theta = \pi/2$), the local Sherwood number or local molar flux is found to be minimum for prolate drop, and maximum for oblate. And at steady-state, the local flux close to the forward stagnation point is higher than close to the end of the drop.

Finally, the total quantity of material transferred to or from the drop, $\overline{Sh}A^*$, has been obtained and presented in terms of the dimensionless shape and time functions. It has been found that the total quantity of material transferred to or from the drop decreases with time and it was determined that when the dimensionless time is greater than 2, then steady-state is, in practice, obtained. Also, prolate drops attain steady-state conditions faster than oblate drops. Furthermore, as the eccentricity increases, the total quantity of material transferred to or from the drop decreases (for a prolate spheroid) and increases (for an oblate spheroid).

Many situations faced in chemical engineering science deal not only with the condition of high Reynolds number but also with the condition of medium and low Reynolds, as well as Peclet numbers. So far, the problem of unsteady mass transfer

presented has been completely investigated at high Peclet numbers for prolate and oblate spheroid in potential flow. As a result, we can extend the work to another axisymmetric body of revolution, such as spherical cap.

References

Abramowitz, M., Stegun, I.A. (1965). *Handbook of Mathematical Functions: with Formulas, Graphs, and Mathematical Tables*. New York: Dover.

Batchelor, G.K. (1967). *An Introduction to Fluid Dynamics.* Cambridge: University-Press.

Bird, R.B., Stewart, W. E., and Lightfoot, E. N. (2002). *Transport phenomena (2nd ed.).* New York: Wiley.

Chao, B.T. (1969). Transient heat and mass transfer to a translating droplet. *Journal of Heat Transfer (Transactions of the ASME)*, **91**, 273-281.

Clift, R., Grace, J.R., and Weber M.E. (1978). *Bubbles, Drops and Particles*. New York: Academic Press.

Favelukis, M., and Semiat, R. (1996). Mass transfer between a slender bubble and a viscous liquid in axisymmetric extensional flow. *Chemical Engineering Science*, 51 , 1169-1172.

Favelukis, M. (1998). Unsteady mass transfer between a slender bubble and a viscous liquid in a simple extensional flow. *Canadian Journal of Chemical Engineering*, **76**, 959-963.

Favelukis M., and Mudunuri R.R. (2003). Unsteady mass transfer in the continuous phase around axisymmetric drops of revolution. *Chemical Engineering Science*, **58**, 1191-1196.

Favelukis M., and Ly C.H. Unsteady mass transfer around spheroidal drop in potential flow. *Chemical Engineering Science*. In press (2005).

Gupalo, I.P., Polianin, A.D., Priadkin, P.A., and Riazantsev, I.S. (1978). On the unsteady mass transfer on a drop in a viscous fluid stream. *Journal of Applied Mathematics and Mechanics* (*PMM*), **42**, 441-449.

Lamb, H. (1945). *Hydrodynamics* (6th ed.). New York: Dover.

Leal, L.G. (1992). *Laminar Flow and Convective Transport Processes: Scaling Principles and Asymptotic Analysis*. Boston: Butterworth-Heinemann.

Levich, V. G. (1962). *Physicochemical Hydrodynamics*. Prentice-Hall, Englewood Cliffs, NJ.

Levich, V.G., Krylov, V.S., and Vorotilin, V.P. (1965). On the theory of unsteady diffusion from moving drops. *Transactions of the Doklady Akademii Nauk SSSR*, **161**, 648-651.

Lochiel, A.C. and Calderbank, P.H. (1964). Mass transfer in the continous phase around axisymmetric bodies of revolution. *Chemical Engineering Science*, **19**, 471-484.

Luiz, A.M. (1967). Drag force on an oblate spheroidal bubble. *Chemical Engineering Science*, **22**, 1083-1090.

Luiz, A.M. (1969). Steady motion of a prolate spheroidal drop. *Chemical Engineering Science*, **24**, 119-123.

Moon P. and Spencer D.E. (1971). *Field Theory Handbook*, 2nd edition, Berlin: Springer-Verlag.

Ruckenstein, E. (1964). On mass transfer in the continuous phase from spherical bubbles or drops. *Chemical Engineering Science*, **19**, 131-146

Ruckenstein, E. (1967). Mass transfer between a single drop and a continuous phase. *International Journal of Heat and Mass Transfer*, **10**, 1785-1792.

Zahm, A.F. (1926). Flow and drag formulas for simple quadrics. *Aerodynamical Laboratory, Bureau of Construction and Repair, U.S. Navy*, Washington, Report 253, 515-537.

Appendix A

Mathematica programs for Chapter 3

A1. Calculation for dimensionless velocity of the prolate spheroid.

A2. Programs for mass transfer calculation.

A1. Calculation for dimensionless velocity of the prolate spheroid

```
(** Calculation for dimensionless velocity in chapter 3.2 **)

Clear[Ao, Bo, A1, B1, ϕ, ϕo, ϕ1, U, d, g, Vθ0, V*, η, ηo, θ];


ϕ[η_, θ_] =
  (Ao + Bo ArcCoth[Cosh[η]]) + (A1 Cosh[η] + B1 (Cosh[η] ArcCoth[Cosh[η]] - 1)) Cos[θ];


ϕo[η_] = Ao + Bo ArcCot[Cosh[η]];


Solve[∂ηo ϕo[ηo] == 0, Bo]

{{Bo → 0}}


Ao = 0;
Bo = 0;
A1 = -U d;


ϕ1[η_, θ_] = (A1 Cosh[η] + B1 (Cosh[η] ArcCoth[Cosh[η]] - 1)) Cos[θ];


Solve[∂ηo ϕ1[ηo, θ] == 0, B1];


Simplify[%]

{{B1 → d U Sinh[ηo]^2 / (-Cosh[ηo] + ArcCoth[Cosh[ηo]] Sinh[ηo]^2)}}


B1 = d U Sinh[ηo]^2 / (-Cosh[ηo] + ArcCoth[Cosh[ηo]] Sinh[ηo]^2);


Vθ0[η_, θ_] = 1 / (d (Sinh[ηo]^2 + Sin[θ]^2)^(1/2)) ∂θ ϕ[ηo, θ];
```

```
Vθ0[η_, θ_] = Simplify[%]
```

$$-\frac{U \sin[\theta]}{\sqrt{\sin[\theta]^2 + \sinh[\eta o]^2}\ (-\cosh[\eta o] + \operatorname{ArcCoth}[\cosh[\eta o]]\ \sinh[\eta o]^2)}$$

```
V*[θ_, e_] = Vθ0[η, θ] / U /. {Sinh[ηo]^2 → 1/e^2 - 1, Cosh[ηo] → 1/e}
```

$$-\frac{\sin[\theta]}{(-\frac{1}{e} + (-1 + \frac{1}{e^2})\ \operatorname{ArcCoth}[\frac{1}{e}])\ \sqrt{-1 + \frac{1}{e^2} + \sin[\theta]^2}}$$

```
Series[V*[θ, e], {e, 0, 1}]
```

$$\frac{3 \sin[\theta]}{2} + O[e]^2$$

```
Series[V*[θ, e], {e, 1, 0}];

Simplify[%, Sin[θ] > 0]
```

$$1 + O[e - 1]^1$$

```
(** Plot Fig 3.2 **)

g = Plot[{3/2 Sin[θ], V*[θ, 0.5], V*[θ, 0.9], V*[θ, 0.99]}, {θ, 0, π}, Frame → True,
  FrameLabel → {FontForm["θ", {"Times", 14}], FontForm["V_θ0 / U", {"Times", 14}]},
  RotateLabel → False, AspectRatio → 3/4, PlotRange → {-0.001, 1.75}]
```

```
- Graphics -
```

```
Show[g, Graphics[{Text["0", {1.575, 1.54}], Text["0.5", {1.575, 1.36}],
   Text["0.9", {1.575, 1.22}], Text["0.99", {1.575, 0.98}]}]]
```

```
- Graphics -
```

A2. Program for mass transfer calculation

```
Clear[Req, R*, d, d*, dx, dx*, Vθ0, V*, m, f, e, θ, t*, ϕ*, Sh, Pe, δR];
<< Graphics`Graphics`
R*[θ_, e_] = (1 - e^2)^(1/6) Sin[θ];
(** dx = d dθ and dx* = d/Req dθ = d* dθ **)
d[θ_, e_] = Req e/(1 - e^2)^(1/3) ((1 - e^2)/e^2 + Sin[θ]^2)^(1/2);
d*[θ_, e_] = d[θ, e]/Req;
Vθ0[θ_, e_] = U Sin[θ]/((1/e^2 - 1 + Sin[θ]^2)^(1/2) (1/e - (1/e^2 - 1) ArcCoth[1/e]));
V*[θ_, e_] = Vθ0[θ, e]/U;
m[θ_, e_] = ∫ d[θ, e]/Vθ0[θ, e] dθ
Req (e + (-1 + e^2) ArcCoth[1/e]) (-e^2 Cos[Θ] + (-1 + e^2) (Log[Cos[Θ/2]] - Log[Sin[Θ/2]]))
e^3 (1 - e^2)^(1/3) U
(** Log[z] gives the natural logarithm of z (logarithm to base e) **)
f[θ_, e_, t* _] = 2 ArcTan[Tan[θ/2] Exp[-e^3 t*/(e - (1 - e^2) ArcCoth[1/e]) (1 - e^2)^(2/3)]];
```

$$\phi^*[\theta\_,\ e\_,\ t^*\_] = \int_f^{\theta} V^*[\theta,\ e]\ (R^*[\theta,\ e])^2\ d^*[\theta,\ e]\ d\theta$$

$$\frac{e^3\ (9\,\text{Cos}[f] - \text{Cos}[3\,f] - 9\,\text{Cos}[\theta] + \text{Cos}[3\,\theta])}{12\ (e + (-1 + e^2)\ \text{ArcCoth}[\frac{1}{e}])}$$

$$\text{Sh} = \frac{1}{\sqrt{\pi}}\ \frac{V^*[\theta,\ e]\ R^*[\theta,\ e]}{\sqrt{\phi^*}}\ \text{Pe}^{1/2}$$

$$\frac{(1 - e^2)^{1/6}\ \sqrt{\text{Pe}}\ \text{Sin}[\theta]^2}{\sqrt{\pi}\ (\frac{1}{e} - (-1 + \frac{1}{e^2})\ \text{ArcCoth}[\frac{1}{e}])\ \sqrt{-1 + \frac{1}{e^2} + \text{Sin}[\theta]^2}\ \sqrt{\phi^*}}$$

$$\delta R = \frac{1}{\text{Sh}\ R^*[\theta,\ e]}$$

$$\frac{\sqrt{\pi}\ (\frac{1}{e} - (-1 + \frac{1}{e^2})\ \text{ArcCoth}[\frac{1}{e}])\ \text{Csc}[\theta]^3\ \sqrt{-1 + \frac{1}{e^2} + \text{Sin}[\theta]^2}\ \sqrt{\phi^*}}{(1 - e^2)^{1/3}\ \sqrt{\text{Pe}}}$$

```
(** Plot Fig 3.3 **)

Clear[f, ϕ*, τ, A, ShPe, ShPea, ShPeb, ShPec, ShPed, g1, g2, g3, g4, f1, f2, f3, f4];

(** t*= τ **)
```

$$f[\theta\_,\ e\_,\ \tau\_] = 2\ \text{ArcTan}\Big[\text{Tan}\Big[\frac{\theta}{2}\Big]\ \text{Exp}\Big[\frac{-e^3\ \tau}{(e - (1 - e^2)\ \text{ArcCoth}[\frac{1}{e}])\ (1 - e^2)^{2/3}}\Big]\Big];$$

$$\phi^*[\theta\_,\ e\_,\ \tau\_] = \int_{f[\theta,e,\tau]}^{\theta} V^*[\theta,\ e]\ (R^*[\theta,\ e])^2\ d^*[\theta,\ e]\ d\theta;$$

$$\text{ShPe}[\theta\_,\ e\_,\ \tau\_] = \frac{1}{\sqrt{\pi}}\ \frac{V^*[\theta,\ e]\ R^*[\theta,\ e]}{\sqrt{\phi^*[\theta,\ e,\ \tau]}};$$

```
ShPea[θ_, τ_] = ShPe[θ, 0.0001, τ];

ShPeb[θ_, τ_] = ShPe[θ, 0.5, τ];

ShPec[θ_, τ_] = ShPe[θ, 0.9, τ];

ShPed[θ_, τ_] = ShPe[θ, 0.99, τ];
```

```
g1 = Plot[{ShPea[θ, 0.01], ShPea[θ, 0.1], ShPea[θ, 1]}, {θ, 10^-2, 3.14}, Frame → True,
   FrameLabel → {FontForm["θ", {"Times", 14}], FontForm["Sh/Pe^1/2", {"Times", 14}]},
   RotateLabel → False, GridLines → Automatic, PlotRange → {-0.001, 8}];

g2 = Plot[{ShPeb[θ, 0.01], ShPeb[θ, 0.1], ShPeb[θ, 1]}, {θ, 10^-2, 3.14}, Frame → True,
   FrameLabel → {FontForm["θ", {"Times", 14}], FontForm["Sh/Pe^1/2", {"Times", 14}]},
   RotateLabel → False, GridLines → Automatic, PlotRange → {-0.001, 8}];

g3 = Plot[{ShPec[θ, 0.01], ShPec[θ, 0.1], ShPec[θ, 1]}, {θ, 10^-2, 3.14}, Frame → True,
   FrameLabel → {FontForm["θ", {"Times", 14}], FontForm["Sh/Pe^1/2", {"Times", 14}]},
   RotateLabel → False, GridLines → Automatic, PlotRange → {-0.001, 8}];

g4 = Plot[{ShPed[θ, 0.01], ShPed[θ, 0.1], ShPed[θ, 1]}, {θ, 10^-2, 3.14}, Frame → True,
   FrameLabel → {FontForm["θ", {"Times", 14}], FontForm["Sh/Pe^1/2", {"Times", 14}]},
   RotateLabel → False, GridLines → Automatic, PlotRange → {-0.001, 8}];

f1 = Show[g1, Graphics[{Text["(a)", {0.2, 7.2}], Text["0.01", {1.575, 6}],
     Text["0.1", {1.575, 2.15}], Text["1", {1.575, 1.2}]}], GridLines → None];

f2 = Show[g2, Graphics[{Text["(b)", {0.2, 7.2}], Text["0.01", {1.575, 5.3}],
     Text["0.1", {1.575, 1.95}], Text["1", {1.575, 1.05}]}], GridLines → None];

f3 = Show[g3, Graphics[{Text["(c)", {0.2, 7.2}], Text["0.01", {1.575, 2.9}],
     Text["0.1", {1.575, 1.2}], Text["1", {0.6, 0.8}]}], GridLines → None];

f4 = Show[g4, Graphics[{Text["(d)", {0.2, 7.2}], Text["0.01", {1.575, 1.2}],
     Text["0.1", {3, 0.5}], Text["1", {0.6, 0.5}]}], GridLines → None];

Show[GraphicsArray[{{f1, f2}, {f3, f4}}]]
```

```
- GraphicsArray -
```

```
(** Sh A* = Sqrt[2/π] h (e) λ (t*,e) Pe^1/2 **)

Clear[h, λ, λ1];

h[e] = 1/Sqrt[2] (∫_0^π V*[θ, e] (R*[θ, e])^2 d*[θ, e] dθ)^1/2

Sqrt[2/3] Sqrt[e^3/(e + (-1 + e^2) ArcCoth[1/e])]
```

```
(** λ(e_,t* _)= λ1(e) ∫_0^π (Sin[θ])^3/√(ϕ*) dθ **)
```

```
V*[θ, e] (R*[θ, e])^2 d*[θ, e];
```

```
Simplify[%]
```

$$\frac{e^3 \text{Sin}[\theta]^3}{e + (-1 + e^2)\,\text{ArcCoth}\left[\frac{1}{e}\right]}$$

```
(** λ[e_,t* _]= ∫_0^π V*[θ,e] (R*[θ,e])^2 d*[θ,e]/√(ϕ*) dθ / (2 (∫_0^π V*[θ,e] (R*[θ,e])^2 d*[θ,e] dθ)^(1/2)) = e^3/(e+(-1+e^2) ArcCoth[1/e]) ∫_0^π (Sin[θ])^3/√(ϕ*) dθ / (2 (∫_0^π V*[θ,e] (R*[θ,e])^2 d*[θ,e] dθ)^(1/2)) **)
```

```
λ1[e_] = e^3/(e+(-1+e^2) ArcCoth[1/e]) / (2 (∫_0^π V*[θ, e] (R*[θ, e])^2 d*[θ, e] dθ)^(1/2));
```

```
Simplify[%]
```

$$\frac{1}{4}\sqrt{3}\,\sqrt{\frac{e^3}{e + (-1 + e^2)\,\text{ArcCoth}\left[\frac{1}{e}\right]}}$$

```
(** Plot Fig 3.4 **)
```

```
Clear[λ, y, gp, gp1];
```

```
λ[e_, τ_] = NIntegrate[V*[θ,e] (R*[θ,e])^2 d*[θ,e]/√(ϕ*[θ,e,τ]), {θ, 0, π}] / (2 (∫_0^π V*[θ, e] (R*[θ, e])^2 d*[θ, e] dθ)^(1/2));
```

```
y[e_, τ_] = √(2/π) h[e] λ[e, τ];
```

```
gp =
 LogLogPlot[{y[10^-5, τ], y[0.5, τ], y[0.9, τ], y[0.99, τ]}, {τ, 10^-3, 10}, Frame → True,
  FrameLabel → {FontForm["t*", {"Times", 14}], FontForm[" Sh A* / Pe^1/2 ", {"Times", 14}]},
  RotateLabel → False, AspectRatio → 3 / 4,
  PlotDivision → 1000, MaxBend → 1, PlotRange → All]
```

```
- Graphics -
```

```
gp1 = Show[gp, Graphics[{Text["0", {-2, 0.8}], Text["0.5", {-2, 0.63}],
     Text["0.9", {-2, 0.415}], Text["0.99", {-2, 0.07}]}]];
```

```
(** short time **)
```

```
Clear[A1, λ];
```

$$(** \lambda[e\_,t^* \_] = \frac{\int_0^{\pi} \frac{V^*[\theta,e]\,(R^*[\theta,e])^2\,d^*[\theta,e]}{\sqrt{\phi^*}}\,d\theta}{2\left(\int_0^{\pi} V^*[\theta,e]\,(R^*[\theta,e])^2\,d^*[\theta,e]\,d\theta\right)^{1/2}} \;\; **)$$

```
A1 = Normal[Series[ϕ*[θ, e, τ], {τ, 0, 1}]];
```

$$\lambda[e\_,\, t^* \_] = \frac{\int_0^{\pi} \frac{V^*[\theta,e]\,(R^*[\theta,e])^2\,d^*[\theta,e]}{\sqrt{A1}}\,d\theta}{2\left(\int_0^{\pi} V^*[\theta,\, e]\,(R^*[\theta,\, e])^2\,d^*[\theta,\, e]\,d\theta\right)^{1/2}};$$

```
Simplify[%]
```

$$\frac{\sqrt{3}\,\sqrt{\frac{e^3}{e+(-1+e^2)\,\text{ArcCoth}\left[\frac{1}{e}\right]}}}{2\,\sqrt{\frac{e^{6\,\tau}}{(1-e^2)^{2/3}\,(e+(-1+e^2)\,\text{ArcTanh}[e])^2}}}$$

Appendix B:

Mathematica programs for Chapter 4

B1. Calculation for dimensionless velocity of the oblate spheroid.

B2. Programs for mass transfer calculation.

B1. Calculation for dimensionless velocity of the oblate spheroid

```
(** Calculation for dimensionlass velocity in chapter 4.2 **)

Clear[Ao, Bo, A1, B1, ϕ, ϕo, ϕ1, U, d, g, Vθ0, V*, η, ηo, θ];


ϕ[η_, θ_] =
  (Ao - Bo i ArcCot[Sinh[η]]) + (A1 i Sinh[η] + B1 (Sinh[η] ArcCot[Sinh[η]] - 1)) Cos[θ];


ϕo[η_] = Ao - Bo i ArcCot[Sinh[η]];


Solve[∂ηo ϕo[ηo] == 0, Bo]

{{Bo → 0}}


Ao = 0;
Bo = 0;
A1 = U d i;


ϕ1[η_, θ_] = (A1 i Sinh[η] + B1 (Sinh[η] ArcCot[Sinh[η]] - 1)) Cos[θ];


Solve[∂ηo ϕ1[ηo, θ] == 0, B1] /. Sinh[ηo]^2 → Cosh[ηo]^2 - 1;


Simplify[%]

{{B1 → d U Cosh[ηo]^2 / (ArcCot[Sinh[ηo]] Cosh[ηo]^2 - Sinh[ηo])}}


B1 = d U Cosh[ηo]^2 / (ArcCot[Sinh[ηo]] Cosh[ηo]^2 - Sinh[ηo]);


Vθ0[η_, θ_] = 1 / (d (Cosh[ηo]^2 - Sin[θ]^2)^(1/2)) ∂θ ϕ[ηo, θ];
```

```
Vθ0[η_, θ_] = Simplify[%]
```

$$\frac{U \sin[\theta]}{\sqrt{\cosh[\eta o]^2 - \sin[\theta]^2}\ (\text{ArcCot}[\sinh[\eta o]]\cosh[\eta o]^2 - \sinh[\eta o])}$$

```
V*[θ_, e_] = Vθ0[η, θ] / U /. {Sinh[ηo] → (1/e^2 - 1)^(1/2), Cosh[ηo] → 1/e}
```

$$\frac{\sin[\theta]}{\left(-\sqrt{-1+\frac{1}{e^2}} + \frac{\text{ArcCot}\left[\sqrt{-1+\frac{1}{e^2}}\right]}{e^2}\right)\sqrt{\frac{1}{e^2} - \sin[\theta]^2}}$$

```
Series[V*[θ, e], {e, 0, 1}]
```

$$\frac{3\sin[\theta]}{2} + O[e]^2$$

```
Series[V*[θ, e], {e, 1, 1}];
```

```
Simplify[%, Sin[θ] > 0]
```

$$-\frac{2\sin[\theta]}{\pi\sqrt{\cos[\theta]^2}} + \frac{16\,i\sin[\theta]\sqrt{e-1}}{\pi^2\sqrt{1+\cos[2\theta]}} - \frac{2\,((2(-8+\pi^2)+(-16+\pi^2)\cos[2\theta])\sin[\theta])(e-1)}{\pi^3(\cos[\theta]^2)^{3/2}} + O[e-1]^{3/2}$$

```
(** Plot Figure 4.2 **)

g = Plot[{3/2 Sin[θ], V*[θ, 0.5], V*[θ, 0.9], V*[θ, 0.99]},
  {θ, 0, π}, Frame → True, PlotRange → {-0.01, 6},
  FrameLabel → {FontForm["θ", {"Times", 14}], FontForm["Vθ0/U", {"Times", 14}]},
  RotateLabel → False, AspectRatio → 3/4]
```

```
- Graphics -
```

```
Show[g, Graphics[{Text["0", {1.575, 1.33}], Text["0.5", {1.575, 1.75}],
   Text["0.9", {1.575, 2.45}], Text["0.99", {1.575, 5.5}]}]]
```

```
- Graphics -
```

B2. Program for mass transfer calculation

```
Clear[Req, R*, d, d*, dx, dx*, Vθ0, V*, m, f, e, θ, t*, ϕ*, Sh, Pe, δR];
<< Graphics`Graphics`
R*[θ_, e_] = (1 - e^2)^-1/6 Sin[θ];
(** dx = d dθ and dx* = d/Req dθ = d* dθ **)
d[θ_, e_] = Req e/(1 - e^2)^1/6 (1/e^2 - Sin[θ]^2)^1/2;
d*[θ_, e_] = d[θ, e]/Req;
Vθ0[θ_, e_] = U Sin[θ]/((1/e^2 - Sin[θ]^2)^1/2 (-(1/e^2 - 1)^1/2 + 1/e^2 ArcCot[(1/e^2 - 1)^1/2]));
V*[θ_, e_] = Vθ0[θ, e]/U;
m[θ_, e_] = ∫ d[θ, e]/Vθ0[θ, e] dθ;
Simplify[%]
```

$$-\frac{\text{Req}\left(\sqrt{-1+\frac{1}{e^2}}\ e^2-\text{ArcCot}\left[\sqrt{-1+\frac{1}{e^2}}\ \right]\right)\left(e^2\,\text{Cos}[\Theta]-\text{Log}\left[\text{Cos}\left[\frac{\Theta}{2}\right]\right]+\text{Log}\left[\text{Sin}\left[\frac{\Theta}{2}\right]\right]\right)}{e^3\,(1-e^2)^{1/6}\,U}$$

```
(** Log[z] gives the natural logarithm of z (logarithm to base e) **)
f[θ_, e_, t* _] = 2 ArcTan[Tan[θ/2] Exp[-e^3 (1 - e^2)^1/6 t*/(-e (1 - e^2)^1/2 + ArcCot[(1/e^2 - 1)^1/2])]];
```

$$\phi^*[\theta\_, e\_, t^*\_] = \int_f^{\theta} V^*[\theta, e]\,(R^*[\theta, e])^2\, d^*[\theta, e]\, d\theta;$$

```
Simplify[%, e > 0]
```

$$\frac{e^3\,(9\,\text{Cos}[f] - \text{Cos}[3\,f] - 9\,\text{Cos}[\theta] + \text{Cos}[3\,\theta])}{12\left(-e + e^3 + \sqrt{1-e^2}\,\text{ArcCot}\left[\sqrt{-1+\frac{1}{e^2}}\,\right]\right)}$$

$$Sh = \frac{1}{\sqrt{\pi}}\,\frac{V^*[\theta, e]\,R^*[\theta, e]}{\sqrt{\phi^*}}\,Pe^{1/2}$$

$$\frac{\sqrt{Pe}\,\text{Sin}[\theta]^2}{(1-e^2)^{1/6}\sqrt{\pi}\left(-\sqrt{-1+\frac{1}{e^2}} + \frac{\text{ArcCot}\left[\sqrt{-1+\frac{1}{e^2}}\,\right]}{e^2}\right)\sqrt{\frac{1}{e^2} - \text{Sin}[\theta]^2}\,\sqrt{\phi^*}}$$

$$\delta R = \frac{1}{Sh\,R^*[\theta, e]}$$

$$\frac{(1-e^2)^{1/3}\sqrt{\pi}\left(-\sqrt{-1+\frac{1}{e^2}} + \frac{\text{ArcCot}\left[\sqrt{-1+\frac{1}{e^2}}\,\right]}{e^2}\right)\text{Csc}[\theta]^3\sqrt{\frac{1}{e^2} - \text{Sin}[\theta]^2}\,\sqrt{\phi^*}}{\sqrt{Pe}}$$

```
(** Plot Fig 4.3 **)

Clear[f, ϕ*, τ, ShPe, ShPea, ShPeb, ShPec, ShPed, g1, g2, g3, g4, f1, f2, f3, f4];

(** t*= τ **)
```

$$f[\theta\_, e\_, \tau\_] = 2\,\text{ArcTan}\left[\text{Tan}\left[\frac{\theta}{2}\right]\text{Exp}\left[-\frac{e^3\,(1-e^2)^{1/6}\,\tau}{-e\,(1-e^2)^{1/2} + \text{ArcCot}\left[\left(\frac{1}{e^2}-1\right)^{1/2}\right]}\right]\right];$$

$$\phi^*[\theta\_, e\_, \tau\_] = \int_{f[\theta, e, \tau]}^{\theta} V^*[\theta, e]\,(R^*[\theta, e])^2\, d^*[\theta, e]\, d\theta;$$

$$ShPe[\theta\_, e\_, \tau\_] = \frac{1}{\sqrt{\pi}}\,\frac{V^*[\theta, e]\,R^*[\theta, e]}{\sqrt{\phi^*[\theta, e, \tau]}};$$

```
ShPea[θ_, τ_] = ShPe[θ, 0.0001, τ];

ShPeb[θ_, τ_] = ShPe[θ, 0.5, τ];

ShPec[θ_, τ_] = ShPe[θ, 0.9, τ];
```

```
ShPed[θ_, τ_] = ShPe[θ, 0.99, τ];

g1 = Plot[{ShPea[θ, 0.01], ShPea[θ, 0.1], ShPea[θ, 1]}, {θ, 10^-2, 3.14}, Frame → True,
   FrameLabel → {FontForm["θ", {"Times", 14}], FontForm["Sh/Pe^1/2", {"Times", 14}]},
   RotateLabel → False, GridLines → Automatic, PlotRange → {-0.001, 8}];

g2 = Plot[{ShPeb[θ, 0.01], ShPeb[θ, 0.1], ShPeb[θ, 1]}, {θ, 10^-2, 3.14}, Frame → True,
   FrameLabel → {FontForm["θ", {"Times", 14}], FontForm["Sh/Pe^1/2", {"Times", 14}]},
   RotateLabel → False, GridLines → Automatic, PlotRange → {-0.001, 8}];

g3 = Plot[{ShPec[θ, 0.01], ShPec[θ, 0.1], ShPec[θ, 1]}, {θ, 10^-2, 3.14}, Frame → True,
   FrameLabel → {FontForm["θ", {"Times", 14}], FontForm["Sh/Pe^1/2", {"Times", 14}]},
   RotateLabel → False, GridLines → Automatic, PlotRange → {-0.001, 14}];

g4 = Plot[{ShPed[θ, 0.01], ShPed[θ, 0.1], ShPed[θ, 1]}, {θ, 10^-2, 3.14}, Frame → True,
   FrameLabel → {FontForm["θ", {"Times", 14}], FontForm["Sh/Pe^1/2", {"Times", 14}]},
   RotateLabel → False, GridLines → Automatic, PlotRange → {-0.001, 42}];

f1 = Show[g1, Graphics[{Text["(a)", {0.2, 7.2}], Text["0.01", {1.575, 6}],
     Text["0.1", {1.575, 2.15}], Text["1", {1.575, 1.2}]}], GridLines → None];

f2 = Show[g2, Graphics[{Text["(b)", {0.2, 7.2}], Text["0.01", {1.575, 6.9}],
    Text["0.1", {1.575, 2.4}], Text["1", {1.575, 1.2}]}], GridLines → None]

- Graphics -

f3 = Show[g3, Graphics[{Text["(c)", {0.2, 12.5}], Text["0.01", {1.575, 11.5}],
    Text["0.1", {1.575, 4.6}], Text["1", {1.575, 2}]}], GridLines → None]

- Graphics -

f4 = Show[g4, Graphics[{Text["(d)", {0.15, 38}], Text["0.01", {1.8, 40}],
    Text["0.1", {1.575, 14}], Text["1", {1.575, 5.9}]}], GridLines → None]

- Graphics -

Show[GraphicsArray[{{f1, f2}, {f3, f4}}]]

- GraphicsArray -

(** Sh̄ A* = √(2/π) h (e) λ (t*, e) Pe^1/2 **)

Clear[h, λ, λ1];
```

$$\mathbf{h[e]} = \frac{\mathbf{1}}{\sqrt{\mathbf{2}}} \left(\int_0^{\pi} \mathbf{V^*[\theta, e]\ (R^*[\theta, e])^2\ d^*[\theta, e]}\ d\theta \right)^{1/2};$$

Simplify[%, e > 0]

$$\sqrt{\frac{2}{3}}\ \sqrt{\frac{e^3}{-e + e^3 + \sqrt{1 - e^2}\ \text{ArcCot}\left[\sqrt{-1 + \frac{1}{e^2}}\right]}}$$

(λ (e,t*)= λ1 (e)** $\int_0^{\pi} \frac{(\text{Sin}[\theta])^3}{\sqrt{\phi^*}}\ d\theta$ ****)**

V*[θ, e] (R*[θ, e])^2 d*[θ, e];

Simplify[%, e > 0]

$$\frac{e^3\ \text{Sin}[\theta]^3}{-e + e^3 + \sqrt{1 - e^2}\ \text{ArcCot}\left[\sqrt{-1 + \frac{1}{e^2}}\right]}$$

(λ[e_,t* _]=** $\frac{\int_0^{\pi} \frac{V^*[\theta,e]\ (R^*[\theta,e])^2\ d^*[\theta,e]}{\sqrt{\phi^*}}\ d\theta}{2\left(\int_0^{\pi} V^*[\theta,e]\ (R^*[\theta,e])^2\ d^*[\theta,e]\ d\theta\right)^{1/2}} = \frac{\frac{e^3}{-e+e^3+\sqrt{1-e^2}\ \text{ArcCot}\left[\sqrt{-1+\frac{1}{e^2}}\right]} \int_0^{\pi} \frac{(\text{Sin}[\theta])^3}{\sqrt{\phi^*}}\ d\theta}{2\left(\int_0^{\pi} V^*[\theta,e]\ (R^*[\theta,e])^2\ d^*[\theta,e]\ d\theta\right)^{1/2}}$ ****)**

$$\lambda\mathbf{1[e\_]} = \frac{\frac{e^3}{-e+e^3+\sqrt{1-e^2}\ \text{ArcCot}\left[\sqrt{-1+\frac{1}{e^2}}\right]}}{2\left(\int_0^{\pi} \mathbf{V^*[\theta, e]\ (R^*[\theta, e])^2\ d^*[\theta, e]}\ d\theta\right)^{1/2}};$$

Simplify[%, e > 0]

$$\frac{1}{4}\ \sqrt{3}\ e^{3/2}\ \sqrt{\frac{1}{-e + e^3 + \sqrt{1 - e^2}\ \text{ArcCot}\left[\sqrt{-1 + \frac{1}{e^2}}\right]}}$$

(Plot Fig 4.4 **)**

Clear[y, λ, gp, gp1];

$$\lambda\mathbf{[e\_,\ \tau\_]} = \frac{\mathbf{NIntegrate}\left[\frac{V^*[\theta,e]\ (R^*[\theta,e])^2\ d^*[\theta,e]}{\sqrt{\phi^*[\theta,e,\tau]}},\ \{\theta,\ 0,\ \pi\}\right]}{2\left(\int_0^{\pi} \mathbf{V^*[\theta, e]\ (R^*[\theta, e])^2\ d^*[\theta, e]}\ d\theta\right)^{1/2}};$$

```
y[e_, τ_] = Sqrt[2/π] h[e] λ[e, τ];
```

```
gp =
 LogLogPlot[{y[10^-5, τ], y[0.5, τ], y[0.9, τ], y[0.99, τ]}, {τ, 10^-3, 10}, Frame → True,
  FrameLabel → {FontForm["t*", {"Times", 14}], FontForm["Sh A*/Pe^1/2", {"Times", 14}]},
  RotateLabel → False, AspectRatio → 3 / 4,
  PlotDivision → 1000, MaxBend → 1, PlotRange → All]
```

```
- Graphics -
```

```
gp1 = Show[gp, Graphics[{Text["0", {-2, 0.68}],
    Text["0.5", {-2, 0.87}], Text["0.9", {-2, 1.08}], Text["0.99", {-2, 1.42}]}]]
```

```
- Graphics -
```

```
(** short time **)
```

```
Clear[A1, λ];
```

$$(**\ \lambda[e\_,t^*\_]=\frac{\int_0^{\pi}\frac{V^*[\theta,e]\,(R^*[\theta,e])^2\,d^*[\theta,e]}{\sqrt{\phi^*}}\,d\theta}{2\left(\int_0^{\pi}V^*[\theta,e]\,(R^*[\theta,e])^2\,d^*[\theta,e]\,d\theta\right)^{1/2}}\ \ **)$$

```
A1 = Normal[Series[ϕ*[θ, e, τ], {τ, 0, 1}]];
```

$$\lambda[e\_,\ t^*\_] = \frac{\int_0^{\pi}\frac{V^*[\theta,e]\,(R^*[\theta,e])^2\,d^*[\theta,e]}{\sqrt{A1}}\,d\theta}{2\left(\int_0^{\pi}V^*[\theta,e]\,(R^*[\theta,e])^2\,d^*[\theta,e]\,d\theta\right)^{1/2}};$$

```
FullSimplify[%]
```

$$\frac{\sqrt{3}\,\sqrt{-\frac{e^3}{\sqrt{1-e^2}\,\left(\sqrt{-1+\frac{1}{e^2}}\,e^2-\text{ArcCot}\left[\sqrt{-1+\frac{1}{e^2}}\right]\right)}}}{2\,\sqrt{\frac{e^6\,\tau}{(1-e^2)^{1/3}\,\left(\sqrt{-1+\frac{1}{e^2}}\,e^2-\text{ArcCot}\left[\sqrt{-1+\frac{1}{e^2}}\right]\right)\,\left(e\,\sqrt{1-e^2}-\text{ArcCot}\left[\sqrt{-1+\frac{1}{e^2}}\right]\right)}}}$$